

1 Impacts of drainage, restoration and warming on boreal wetland greenhouse gas
2 fluxes

3 Laine, A.M.^{1,2,3*}, Mehtätalo, L.⁴, Tolvanen, A.^{2,5} Frohking, S^{3,6}, Tuittila, E.-S.³

4 ¹Department of Forest Science, University of Helsinki, P.O. Box 27, FI-00014 University of
5 Helsinki, Finland;

6 ²Department of Ecology and Genetics, University of Oulu, P.O. Box 3000, FI-90014
7 University of Oulu. Fax +358 8 553 1061

8 ³School of Forest Sciences, University of Eastern Finland, P.O. Box 111, FI-80101 Joensuu,
9 Finland; eeva-stiina.tuittila@uef.fi

10 ⁴School of Computing, University of Eastern Finland, P.O. Box 111, FI-80101 Joensuu,
11 Finland; lauri.mehtatalo@uef.fi

12 ⁵Natural Resources Institute Finland (Luke), P.O. Box 413, FI-90014 University of Oulu,
13 Finland; anne.tolvanen@luke.fi

14 ⁶Institute for the Study of Earth, Oceans, and Space, University of New Hampshire, 8 College
15 Road, Durham, NH 03824-3525, USA; steve.frohking@unh.edu

16 *Corresponding author: Current address, School of Forest Sciences, University of Eastern
17 Finland, P.O. Box 111, FI-80101 Joensuu, Finland; anna.laine@oulu.fi

18

19 To be submitted to Science of the total environment as a Primary Research Article

20 Running head: land use and warming impacts gas fluxes

21 Abstract

22 Northern wetlands with organic soil i.e., mires are significant carbon storages. This key
23 ecosystem service may be threatened by anthropogenic activities and climate change, yet we
24 still lack a consensus on how these major changes affects their carbon sink capacities. We
25 studied how forestry drainage and restoration combined with experimental warming, impacts
26 greenhouse gas fluxes of wetlands with peat. We measured CO₂ and CH₄ during two and N₂O
27 fluxes during one growing season using the chamber method.

28 Gas fluxes were primarily controlled by water table, leaf area and temperature. Land use had
29 a clear impact of on CO₂ exchange. Forestry drainage increased respiration rates and
30 decreased field layer net ecosystem CO₂ uptake (NEE) and leaf area index (LAI), while at
31 restoration sites the flux rates and LAI had recovered to the level of undrained sites. CH₄
32 emissions were exceptionally low at all sites during our study years due to natural drought,
33 but still somewhat lower at drained compared to undrained sites. Moderate warming triggered
34 an increase in LAI across all land use types. This was accompanied by an increase in
35 cumulative seasonal NEE. Restoration appeared to be an effective tool to return the
36 ecosystem functions of these wetlands as we found no differences in LAI or any gas flux
37 components (P_{MAX}, Reco, NEE, CH₄ or N₂O) between restored and undrained sites. We did
38 not find any signs that moderate warming would compromise the return of the ecosystem
39 functions related to C sequestration.

40

41 Keywords: forestry drainage, greenhouse gas, land use, peatland, restoration, open top
42 chamber

43

44 1. Introduction

45 Northern wetlands with organic soil i.e., mires have accumulated a large quantity of peat,
46 accounting for some 30% of global soil carbon (e.g. Yu, 2012). In general, mires have had a
47 small net cooling effect on climate over the Holocene (Frolking, Roulet 2007). Although
48 most undisturbed mires currently act as CO₂ sinks (e.g. Lund et al. 2010) and CH₄ sources
49 (e.g. Lai 2009) to the atmosphere, it is highly uncertain whether mires have a positive or
50 negative feedback in response to global change (Meng et al. 2016). Moreover, this ecosystem
51 function (i.e., carbon sequestration) that mires provide is sensitive to climate variability
52 (Turetsky et al. 2008) and land use change (Ojanen et al., 2013; Renou-Wilson et al. 2014).
53 Utilization of mires for food or timber production usually requires drainage, as the shallow
54 aerobic surface layer of undrained mires is inadequate to support profitable timber or crop
55 growth (Paavilainen, Päivänen 1995). Altogether 30 Mha of non-tropical and 20 Mha of
56 tropical mires have been disturbed by human activities (Joosten 2010), and of this,
57 approximately half has been drained for forestry (Paavilainen, Päivänen 1995; Miettinen et al.
58 2016). Forestry drainage causes a regime shift from open mires towards forests as it alters the
59 hydrology, increases the aeration of peat and redirects the vegetation succession towards
60 forest species (Laine et al. 1995; Vompersky, Sirin 1997; Mälson et al. 2008). Drainage
61 increases decomposition and therefore CO₂ efflux, while CH₄ emissions usually decrease. In
62 most cases, the increased respiration rates are not exceeded by increased productivity and
63 therefore drained mires functions as C sources and have a climate warming impact (Maljanen
64 et al. 2010; Ojanen et al. 2013; Renou-Wilson et al. 2014; Jauhiainen et al. 2016). There are
65 indicators that some nutrient poor forestry drained mires may continue to act as carbon sinks,
66 however (e.g. Lohila et al. 2011; Ojanen et al. 2013; Hommeltenberg et al. 2014; Ojanen et
67 al. unpublished data). In addition to CO₂ and CH₄, nitrous oxide is a strong potent GHG.
68 Generally, N₂O emissions from pristine mires are low and insignificant, but may increase

69 significantly after drainage, especially with more nutrient rich conditions (Regina et al. 1996;
70 Ojanen et al. 2010; Pearson et al. 2015).

71

72 Ecological restoration aims to assist the recovery of an ecosystem that has been degraded,
73 damaged, or destroyed (Hobbs, Cramer 2008) and recent global and national policies (EU
74 Biodiversity Strategy to 2020; Aichi Biodiversity Targets 2011) regard restoration as a
75 crucial means to safeguard biodiversity. Mire restoration has also been promoted as a key
76 climate mitigation tool (e.g. Bonn et al., 2014), and as a means to decrease a country's
77 greenhouse gas (GHG) emissions (IPCC, 2013). At the same time, carbon markets have been
78 identified as possible funding sources for mire restoration schemes (Bonn et al. 2014).
79 However, data on GHG fluxes from restored mires, especially from those restored after
80 drainage for forestry, are very limited.

81

82 The principal restoration methods for forestry drained boreal mires are the blocking of
83 ditches to re-create the high water table level, and the removal of excess trees to reduce the
84 transpiration rate and reinstate the landscape typical of natural mires (e.g., Tarvainen et al.,
85 2013). Most research on mire restoration has concentrated on the restoration of peat
86 harvesting areas, which presents quite a different starting point for restoration compared to
87 forestry drainage (Chimner et al. 2017). The few existing studies on C gas fluxes or carbon
88 accumulation rates on restored peat harvesting areas (e.g. Tuittila et al. 1999; Waddington et
89 al. 2010; Strack, Zuback, 2013; Wilson et al. 2016) and forestry drained mires (Komulainen
90 et al. 1998, 1999; Urbanová et al. 2012; Kareksela et al. 2015; Koskinen et al. 2016) indicate
91 that the rising water table increases the rate of field layer photosynthesis, decreases CO₂
92 efflux and increases CH₄ emissions, thereby partially or fully restoring natural mire functions.

93

94 Projected global warming in northern latitudes (IPCC 2013) is going to have its own impact
95 on mire GHG exchange. Experimental warming studies on mires have been carried out with
96 increasing frequency since 2000 (e.g. Wiedermann et al. 2007; Turetsky et al. 2008;
97 Dorrepaal et al. 2009; Chivers et al. 2009; Johnson et al. 2013; Ward et al. 2013; Munir,
98 Strack 2014; Pearson et al. 2015; Peltoniemi et al. 2016; Voigt et al. 2017; Gill et al. 2017;
99 Mäkiranta et al. 2018). These studies, which mostly use open top chambers (OTC's), have
100 shown varied responses of vegetation, microbial communities and gas fluxes to warming
101 within a few years' study periods. In most cases warming has increased respiration, but the
102 impact on photosynthesis and methane emissions has been context dependent and strongly
103 influenced by species composition and water table level: under wet conditions these fluxes
104 may increase, while, under dry conditions and lower water table, in most cases,
105 photosynthesis and methane emissions either decrease or remain unchanged (Turetsky et al.
106 2008; Dorrepaal et al. 2009; Ward et al. 2013; Munir, Strack 2014; Pearson et al. 2015;
107 Peltoniemi et al. 2016; Gill et al. 2017; Voigt et al. 2017). Denitrification and consequently
108 N₂O fluxes have high temperature sensitivity (Butterbach-Bahl et al. 2013) due to which
109 warming should increase N₂O emissions. This far there have been only a few studies
110 including warming impacts on N₂O emission, and in these, either no changes (Ward et al.
111 2013, Pearson et al. 2015) or increased emissions (Voigt et al. 2017) have been observed.
112 Further, how warming impacts GHG exchange under different land uses
113 (drainage/restoration) have not been documented in mires thus far.

114

115 Our aim is to quantify how forestry drainage and restoration impact GHG dynamics and
116 whether the effects of moderate warming differ between the land uses. To tease out the direct

117 impact of warming we measured CO₂, CH₄ and N₂O fluxes, and leaf area development at six
118 wetlands with peat or primary mires (sensu Joosten et al. 2017) over two growing seasons.
119 Primary mires are successional young wetlands that, under suitable climatic conditions, will
120 develop into deep peat mires (Tuittila et al. 2013; Joosten et al. 2017) and they are known to
121 rapidly respond to climatic variation (Laitinen et al. 2008; Leppälä et al. 2011a). Four of the
122 sites have experienced long-term water table drawdown due to ditching for forestry in the
123 1970s, while restoration of two of these sites in 2008 raised water table levels back to the same
124 level as in the two undrained (control) sites (see Laine et al. 2016). Open top chambers (OTC)
125 were used to warm the plots.

126

127 We hypothesized that 1) drainage increases CO₂ and N₂O release and decreases CH₄ emissions
128 in comparison to undrained sites. 2) Restoration returns ecosystem functions back to the level
129 of undrained sites rapidly (< 5 years); this means that the restored sites are CO₂ sinks, CH₄
130 emitters and have very low N₂O emissions. 3) Warming promotes ecosystem respiration but
131 the response of photosynthesis and methane emissions depends on the prevailing hydrology;
132 under undrained and restored conditions warming increases photosynthesis and methane
133 emissions, but under drained conditions these functions remain unchanged. 4) Warming
134 promotes N₂O emissions.

135

136 **2. Material and methods**

137 **2.1. Study area**

138 The study was carried out on the Finnish coast of the Gulf of Bothnia in Siikajoki (drained
139 and restored sites: ~64°48'93N, 24°37'39E; undrained sites: 64°46'91N, 24°38'65E). We

140 selected six primary mires belonging to three land use categories: two undrained (UD1,
141 UD2), two forestry drained in 1970's (D1, D2), and two drained (1970's) sites restored in
142 2008 (R1, R2). The drainage of site D2 had not resulted in effective regime shift towards
143 forested ecosystem, and the water table was clearly higher than at D1 (see Laine et al. 2016).
144 Restoration was carried out by felling most trees so that ~0–5 trees were left per 100 m², and
145 blocking ditches with soil excavated near the ditches. The sites have been formed in the coast
146 following post-glacial land uplift approximately 100-200 years ago (Ekman 1996). They are
147 located 1.5 - 2 m above sea level in small (~0.5-3 ha) depressions between nutrient-poor sand
148 dunes. The organic soil layer laying over sand is only 5-10 cm thick and the organic matter
149 content of the top 10 cm at the undrained sites varies from 25 to 46 %, with pH of 6.3 to 6.6
150 (Merilä et al. 2006). The sand underneath the organic soil has aeolian origin, it is nutrient
151 poor and has particle size of ~0.17 mm (Hellemaa 1998). The length of growing season in the
152 area is 150 days, the 30-yr average annual temperature 2.6 °C, and the average annual
153 precipitation 541 mm (Revonlahti weather station, Siikajoki, 64° 41'N, 25° 05'E, 48 m a.s.l.;
154 Pirinen et al. 2012; see Table 1 for more climate details).

155

156 Based on differences in tree stand and hydrology, the originally drained sites were divided
157 into two groups. Sites D1 and R1 (group 1) had successful drainage results with clearly
158 increased tree growth, while sites D2 and R2 (group 2) had only sparse tree stands.
159 Additionally, the undrained control sites were assigned into these two groups but based on
160 their terrestrial age, so that the younger site (age ~100 yr), UD1, was assigned to group 1 and
161 the slightly older site (age ~150 yr), UD2, to group 2. The undrained sites are open treeless
162 wetlands with the field layer (including small shrubs, herbaceous plants and moss layer) plant
163 community composed of graminoids (*Carex nigra*, *C. canescens*) and forbs (*Comarum*
164 *palustre*, *Equisetum fluviatile*, *Peucedanum palustre*). The moss layer is composed mainly of

165 *Warnstorfia exannulata* and *Calliergon* species, while some patches of *Sphagnum* mosses
166 (e.g. *S. squarrosum*, *S. fimbriatum*) can also be found. At drained sites, the field layer
167 vegetation is dominated by shrubs (*Vaccinium uliginosum*, *V. vitis-idaea*, *Salix repens*) and
168 feather mosses (*Pleurozium shreberii*, *Polytrichum commune*), although at D2 sedges (*Carex*
169 *nigra*, *C. canescens*) are also abundant. The restored sites are open, with only few scattered
170 trees; at the field layer sedges (*Carex nigra*, *C. canescens*) form the majority of the
171 vegetation and shrubs (e.g. *Salix repens*) are common. Moss layer is sparse and *Warnstorfia*
172 *exannulata* occurs with remnants of e.g. *Pleurozium schreberi* and *Polytrichum strictum*. For
173 more details on vegetation composition, see Laine et al. (2016).

174

175 At each site, we established ten permanent sample plots and assigned half of them to a
176 warming experiment, covering them with open top chambers (OTC). OTC is a passive
177 warming method that aims at a moderate warming impact of 1-3 °C. The remaining five plots
178 at each site are the ambient temperature (ambient-T) plots. The first set of OTCs was installed
179 in autumn 2008 to sites UD2, D2 and R2 and the second set was installed in spring 2011 to
180 sites UD1, D1 and R1. The OTCs were constructed from durable transparent polycarbonate
181 and had a projected area of 1.5 m² (see Pearson et al. 2015). They were removed from the
182 plots during the typical snow-covered period (November-April) to maintain natural snow
183 cover. Soil temperature at 5 and 15 cm depth and air temperature at 30 cm height were
184 monitored continuously within each sample plot at 2h time step during the snow free period
185 (iButton, Maxim Integrated, U.S.). At the beginning of May 2011, a month before the first
186 gas flux measurements, square aluminium collars (58 x 58 cm) were permanently inserted
187 into sample plots to support gas flux measurements. The collar rim reached about 15 cm into
188 the soil, but the deeper roots of trees and vascular plants were left intact. Sample plots were
189 surrounded by boardwalk platforms to avoid trampling.

190

191 **2.2. Field measurements**

192 We performed weekly to biweekly CO₂ flux measurements from June to November in 2011
193 and from May to November in 2013, i.e. three and five years after restoration. Monthly
194 methane (CH₄) fluxes were measured from May - September 2011 and June to August 2013.
195 Monthly nitrous oxide (N₂O) fluxes were measured from May to September 2011. Seasonal
196 development of field layer leaf area index (LAI) was monitored during the 2011 and 2013
197 growing seasons. To facilitate gas flux measurements, the OTC's were lifted up from the
198 warmed plot for the duration of the measurement (15 to 30 minutes).

199

200 **CO₂ flux** was measured with a transparent plastic chamber (60x60x30 cm) that was
201 connected to a portable infrared gas analyser (EGM-4, PP Systems, UK). The chamber was
202 equipped with a fan and a cooling system that maintained the air temperature within 2°C of
203 ambient (Alm et al. 2007). Two to three study sites were measured within the same day,
204 typically between 9 a.m. and 5 p.m. At each sample plot measurements were made under
205 ambient stable light, with the chamber shaded by a mesh fabric to decrease the photosynthetic
206 photon flux density (PPFD) level, and with chamber covered by an opaque shroud (PPFD 0).
207 Each measurement lasted 90-180s. The chamber was lifted and ventilated between
208 measurements to restore the ambient CO₂ concentration. During the measurements,
209 headspace CO₂ concentration, photon flux density (PPFD) and chamber temperature were
210 recorded at 15s intervals.

211

212 The net ecosystem CO₂ exchange (NEE) was calculated from the linear change in CO₂
213 concentration in chamber headspace, as a function of the chamber headspace volume and
214 mean chamber air temperature during the measurement. Dark measurements were used as an
215 estimate of instantaneous ecosystem respiration (Reco). Gross photosynthesis (PG) was
216 calculated by subtracting NEE rate measured in full light and shaded conditions from the
217 subsequent dark measurement (e.g. Alm 2007). Our sign convention shows positive NEE
218 when the ecosystem is a CO₂ sink from the atmosphere.

219

220 **Methane (CH₄) and nitrous oxide (N₂O) fluxes** were measured with opaque chambers
221 (60x60x30cm), equipped with fans for air circulation. Four 60 ml gas samples were taken
222 from the chamber with plastic syringes at 5, 15, 25 and 35 minutes after closure. Samples
223 were stored in 12 ml glass vials until analysis. Chamber headspace temperature was
224 monitored during measurements.

225

226 Samples from 2011 were analysed for CH₄ and N₂O in the Natural Resources Institute of
227 Finland laboratory at Vantaa, using an Agilent Technologies 7980A gas chromatograph.
228 Samples from 2013 were analysed for CH₄ at the Hyytiälä Forestry Field Station, Finland,
229 using a HP-5890A gas chromatograph. CH₄ and N₂O fluxes were calculated from the linear
230 change in chamber headspace gas concentration as a function of headspace area, volume and
231 mean headspace temperature during the measurement. The correlations (r^2) of the linear
232 change in gas concentrations were generally above 0.9 and 0.8 for CH₄ and N₂O respectively;
233 however, when flux rates were near zero (ranging from -0.05 – +0.03 mg m⁻² h⁻¹), lower r^2
234 were typical and these fluxes were not rejected. We rejected only the measurements that
235 where clearly non-linear, without being near zero, altogether 2% of the measurements.

236

237 Field layer vascular plant **leaf area index (LAI)** was measured six and seven times during
238 years 2011 and 2013, respectively. Within each sample plot, five 8*8 cm sub-plots were
239 established and the number of leaves of each vascular plant species was counted every three
240 weeks. At the same time leaves of each species were collected outside the gas flux plots,
241 carefully mounted on paper and scanned. Leaf area was digitally analysed from the images.
242 We calculated LAI of each species as a product of the number of leaves and the average leaf
243 size. Seasonal LAI development was estimated with statistical modelling, see section 2.4.1.

244

245 **Supporting measurements** of soil temperature and water table level were made during gas
246 flux campaigns. During flux measurements, we manually measured soil temperature at 5, 10
247 and 15 cm depth next to each sample plot and measured water table level using perforated
248 pipes that were inserted into the soil at close vicinity of the sample plots. Soil or moss surface
249 was used as the zero reference level.

250

251 **2.3. Carbon sequestration of the tree stand**

252 Tree stand characteristics were measured in 2005, 2009 and 2013 at 12 and 14 permanent
253 circular plots at sites all sites. The number of all trees taller than 1.3 m and diameter at breast
254 height (D_{bh}) more than 45 mm was counted and D_{bh} of all trees was measured. For each
255 species we chose the tree with largest D_{bh} and at least one tree from diameter classes 10 - 20
256 cm and 4.5 – 10 cm as sample trees. From these sample trees height (h) and living crown
257 length and width were measured. Based on these data we calculated the stand density (trees
258 ha^{-1}) and annual volume increment with the KPL software (Heinonen, 1994).

259

260 While the tree stand of undrained and restored sites was either absent or minor, at drained
261 sites the carbon sequestration of the tree stand was estimated as follows: To calculate the
262 above- and belowground biomass for birches and pines separately, we used species-specific
263 models developed by Repola, (2008; 2009). Above ground biomass estimates were based on
264 D_{bh} and tree height, while the below ground biomass estimates were based on D_{bh} . The tree
265 stand biomass difference between years 2013 and 2005 was used to calculate the annual
266 biomass increment and converted it to carbon using the frequently applied conversion factor
267 0.50 (see e.g. Laiho, Laine 1997).

268

269 **2.4. Data analysis**

270 We applied linear and nonlinear hierarchical mixed-effects modelling to quantify how long-
271 term drainage, restoration and moderate warming impact LAI development and GHG flux
272 dynamics of the field layer of the primary mires. We used two steps in the gas flux
273 modelling. First, we related gas flux parameters (e.g. P_{MAX} and Reco, see Eq. 4 below) to
274 so-called stable factors, namely land use category, warming treatment, year and site group
275 (group 1: UD1, D1 and R1; group 2: UD2, D2 and R2). Then we built so-called “full models”
276 that also included environmental variables (temperature, LAI etc.) as explanatory variables of
277 the gas flux parameters. The model building was based on known properties of the natural
278 process, where the effects of treatments and environmental factors on the model parameters
279 were concurrently analysed and added sequentially to the model in order of importance. The
280 prediction of the LAI model is included as an environmental variable in the CO₂ and CH₄
281 models.

282

283 2.4.1. LAI modelling

284 Seasonal LAI development can be described with a log-normal unimodal function with
285 parameters for maximum leaf area ($LMAX_{ijk}$) and timing of maximum leaf area ($DMAX_{ijk}$).

286 Our modelling procedure follows that presented by Mäkiranta et al. (2017).

$$287 \quad y_{ijkl} = LMAX_{ijk} \times \exp \left[-0.5 \left(\frac{\log \left(\frac{T_{ijkl}}{DMAX_{ijk}} \right)}{G_{ijk}} \right)^2 \right] + e_{ijk}; \quad LMAX_{ijk}, DMAX_{ijk}, G_{ijk} > 0 \quad (1)$$

288 where y_{ijkl} is the observed LAI ($m^2 m^{-2}$) at light level l within year k within plot j within site i ,
289 and the predictor T_{ijkl} is the corresponding Julian days since the beginning of year. The
290 parameters of the model are the maximum LAI ($LMAX_{ijk}$), its timing ($DMAX_{ijk}$), and the
291 scale parameter G_{ijk} , which is related to the temporal scale of LAI development. The
292 residuals (e_{ijk}) did not show signs of inconstant variability and temporal autocorrelation, and
293 it was therefore assumed that they are independent with zero mean and common variance
294 (σ^2). To quantify the impacts of treatments on the LAI parameters, they were further written
295 as linear functions of fixed predictors (land use, warming, year and site group) and three
296 nested random effects for site, plot within site, and year within plot within site. Logarithmic
297 form was used to ensure positive values of parameters in all cases. The resulting submodels
298 are:

$$299 \quad LMAX_{ijk} = \exp(\beta^{LMAX} \cdot \mathbf{x}_{ijk}^{LMAX} + a_i^{LMAX} + b_{ij}^{LMAX} + c_{ijk}^{LMAX}) \quad (2)$$

$$300 \quad DMAX_{ijk} = \exp(\beta^{DMAX} \cdot \mathbf{x}_{ijk}^{DMAX} + a_i^{DMAX} + b_{ij}^{DMAX} + c_{ijk}^{DMAX}) \quad (3)$$

$$301 \quad G_{ijk} = \exp(\beta^G \cdot \mathbf{x}_{ijk}^G + a_i^G + b_{ij}^G + c_{ijk}^G) \quad (4)$$

302 where the inner product $\beta^{LMAX} \cdot x_{ijk}^{LMAX}$, $\beta^{DMAX} \cdot x_{ijk}^{DMAX}$ and $\beta^G \cdot x_{ijk}^G$ include the fixed effects
303 of the treatments on LMAX and DMAX (the terms included in the final models will be
304 shown in result tables). The normally distributed random effects for different parameters at
305 the same level (e.g. a_i^{LMAX} , a_i^{DMAX} , a_i^G) were assumed to be uncorrelated to achieve
306 convergence (Pinheiro and Bates 2000). They modelled the variability that was not explained
307 by the fixed effects, and simultaneously the dependence due to grouping in the data.
308 Submodels (2 and 3) were included in Equation 1 and the resulting model was fitted in one
309 step. We used approximate conditional F- tests (Pinheiro, Bates 2000) and Akaike
310 information criterion (AIC) in model selection. Models were fitted using the nlme package of
311 R (R Core Team 2016), following Pinheiro and Bates (2000). To facilitate CH₄ flux
312 modelling, we also used the same method to model the LAI of species with aerenchyma
313 (mainly sedges in our sites) (LAI_S). See Supporting information 1 for model details.

314 **2.4.2. CO₂ flux modelling**

315 To determine the effects of land use and warming on the light response parameters of
316 photosynthesis, and their dependences to environmental factors (LAI, air temperature, soil
317 temperature) we applied a nonlinear mixed-effects model with the hyperbolic light saturation
318 curve (e.g. Lappi, Oker-Blom 1992):

$$319 \quad A_{ijklm} = R_{ecoijkl} + \frac{P_{MAXijkl} PPF_{Dijklm}}{\alpha_{ijkl} + PPF_{Dijklm}} + e_{ijklm} \quad (4)$$

320 where the response A_{ijklm} is the observed NEE (mg m⁻² h⁻¹), and the predictor PPF_{Dijklm} is the
321 photosynthetic photon flux density (μmol m⁻² s⁻¹) on measurement m of day l of year k of plot
322 j at site i . The parameters to be estimated are respiration ($R_{ecoijkl}$), photosynthetic capacity
323 i.e. the maximum rate of light-saturated gross photosynthesis ($P_{MAXijkl}$) and the maximum
324 quantum yield of CO₂ assimilation (α_{ijkl}), i.e., light use efficiency at low light. The residual
325 (e_{ijklm}) is normally distributed with mean zero and constant variance. Parameters $P_{MAXijkl}$,

326 $Reco_{ijkl}$ and α_{ijkl} were written as linear functions of fixed predictors and random effects. These
 327 submodels are:

$$328 \quad PMAX_{ijkl} = \exp(\beta^{PMAX} \cdot \mathbf{x}_{ijkl}^{PMAX} + a_i^{PMAX} + b_{ij}^{PMAX} + c_{ijk}^{PMAX} + d_{ijkl}^{PMAX}) \quad (5)$$

$$329 \quad Reco_{ijkl} = \exp(\beta^R \cdot \mathbf{x}_{ijkl}^R + a_i^R + b_{ij}^R + c_{ijk}^R + d_{ijkl}^R) \quad (6)$$

$$330 \quad \alpha_{ijkl} = \exp(\beta^\alpha \cdot \mathbf{x}_{ijkl}^\alpha + a_i^\alpha + b_{ij}^\alpha + c_{ijk}^\alpha + d_{ijkl}^\alpha) \quad (7)$$

331

332 The random effects ($a_i^{PMAX} + b_{ij}^{PMAX}, \dots, c_{ijk}^\alpha + d_{ijkl}^\alpha$) were assumed to have mean zero and
 333 common variance; the effects for different parameters at the same level were assumed to be
 334 uncorrelated. In practice, the model building started with a model without predictors and with
 335 random effects d_{ijkl} only. The predictor that showed strongest relationship with the random
 336 effects was thereafter included in the fixed part using appropriate transformation and the
 337 model was re-estimated. The random effects of the updated model were extracted and their
 338 relationship was again explored against the current and potential new predictors. These steps
 339 were iterated until the random effects did not show any unexplained trends. The final model
 340 was then fitted using the above-specified full random effect structure and the fixed effects
 341 were tested using conditional approximate F- tests on the fixed effects ($p > 0.05$). The
 342 number of replicates in our data is small, and therefore the effects of land use or warming
 343 needs to be very large to become statistically significant. To maximally utilize our data and
 344 provide essential information for future research efforts, we therefore report parameter
 345 estimates from the full model and their confidence intervals regardless of their p-values, as in
 346 Mäkiranta et al. (2017).

347

348 To separate the impacts of land use category and warming treatments from those of
 349 environmental variables, we used two sets of fixed predictors (e.g. $\beta^{PMAX} \cdot \mathbf{x}_{ijkl}^{PMAX}$) in the sub-
 350 models (eq. 5-7). The first set included only categorical treatment effects, while the second

351 set also included environmental variables. For the first set, the categorical predictors were
352 land use, warming, measurement year and site group. For the second set, the following
353 environmental variables and their transformations were included to form the full model of
354 $PMAX_{ijkl}$: LAI was included as transformation $LAI_2 = \ln(1 - \exp(-LAI))$ to take into account
355 the self-shading of leaves through Beer-Lambert's law (Wilson 1959). Air temperature was
356 included using a three-knot spline, with knots placed at 15°C, 20°C and 25°C (Harrell 2001),
357 which allowed an optimum temperature within the range of observations (0 – 37°C). The full
358 model of R_{ijkl} included the predicted plot-specific LAI from model (1) in logarithmic form,
359 i.e., respiration was assumed to be linearly related to LAI. Air temperature was used in linear
360 form, which implies an exponential response of respiration to temperature. In addition to air
361 temperature, 15-cm soil temperature was included in the R_{ijkl} models in form with a minimum
362 at 10°C, which allows exponential response to soil temperatures below 10°C. For the
363 submodel of parameter α_{ijkl} (eq. 7), only land use category was used as a fixed predictor. The
364 chosen transformations provided better fits to the data than non-transformed or
365 logarithmically transformed predictors, and satisfactorily modelled all clear trends from the
366 random effects. See Supporting information 2 for model details.

367

368 **2.4.3. CH₄ and N₂O flux modelling:**

369 We used linear mixed-effects models to analyze the effects of land use and warming on CH₄
370 and N₂O fluxes, and their dependences on environmental variables. Inverse transformation,
371 $1/(CH_4 + 0.3)$, was used for CH₄ to homogenize the residual variance of the model (Appendix
372 3). Similar to CO₂ modelling, in the first CH₄ and N₂O modelling steps we included
373 categorical treatment effects as fixed predictors. These were land use category, warming,
374 their interaction, year and site group. In the second step, we formed the full model that also

375 includes environmental variables. For CH₄ flux, the full model included sedge LAI (LAI_S),
376 air temperature (Ta), soil temperature at 5 cm (T5) and water table depth (WT), which was
377 included using a three-knot spline, with knots placed at values -55, -40 and -25 cm (Harrell
378 2001), which allowed an optimum water table within the range of observations (-80 cm – 0
379 cm). For N₂O flux, the full model included total LAI, WT, Ta and T5. Random intercepts
380 were assumed for levels site and plot and measurement time. The plots were nested within
381 sites and crossed with measurement time. See Supporting information 3 and 4 for model
382 details.

383

384 **2.5. Reconstructing seasonal cumulative gas fluxes**

385 We used the fixed part of the full models of CO₂ (eq. 4-7) and CH₄, described earlier, to
386 estimate the seasonal cumulative fluxes of NEE and CH₄. Reconstructions were made with
387 hourly time step and results are reported per square meter. The environmental data for
388 reconstructions was attained as follows: hourly values of PPFD from the Siikajoki, Ruukki
389 weather station (64°68'N, 25°09'E, Finnish Meteorological Institute). PPFD under the forest
390 canopy in site D1 was estimated as in Badorek et al. (2011). Tree canopy leaf area (CLAI) for
391 the calculations was estimated using the biomass equations of Repola (2008, 2009) for Scots
392 pine and birch, and the specific leaf areas of 11 m² kg⁻¹ DW for pine (Luoma 1997), and 25
393 m² kg⁻¹ DW for birch (Parviainen 1999). Soil temperature at 5 and 15 cm depth and air
394 temperature at 30 cm height were continuously recorded beside each sample plot at 2h time
395 step (iButton, Maxim Integrated, U.S.) and interpolated to hourly values, and averages of
396 warmed and ambient-T plots were calculated for each site. Water table was measured during
397 gas flux campaigns, on average once per week. This data was linearly interpolated into hourly

398 values and site averages were calculated. Hourly LAI was predicted using the fixed part of
399 the LAI model for warming and ambient-T plots of each site.

400

401 We reconstructed fluxes for 1 May to 30 September. We had continuous environmental data
402 from 10 May to 30 September for 2011 and from 14 May to 30 September for 2013. For the
403 beginning of May, we multiplied the average May flux rate by the number of missing hours.
404 We acknowledge that gas exchange occurs also during time period not included here. As N₂O
405 flux rates per site were rather constant and not explained by any environmental variable, we
406 estimated the seasonal cumulative flux by multiplying the average flux rate by the number of
407 hours during 1 May to 30 September.

408 **Global warming potentials (GWP)**

409 In order to compare the GHG balance of the different land uses, we calculated the GWP's for
410 each site for growing seasons 2011 and 2013, based on a 100-year time horizon. We used the
411 cumulative seasonal NEE, CH₄ and N₂O fluxes calculated per site and included the carbon
412 sequestration of the tree stand in the NEE of drained sites by adding the estimated annual
413 CO₂ sequestration. GWP's were not calculated for the warming treatment plots as those
414 would not include the response of tree stand to warming. In addition, the N₂O flux estimates
415 from season 2011 were used for 2013. The cumulative seasonal CO₂, CH₄ and N₂O flux
416 estimates were multiplied by 1, 28 and 265, respectively to convert all to CO₂-equivalent
417 fluxes that can be summed (Myhre et al 2013). Negative GWP values indicate a net cooling
418 effect on the climate and positive values indicate a net warming effect.

419

420 **3. Results**

421 **3.1.Environmental conditions**

422 The average WT in the undrained sites was -8 and -27 cm, in the restored sites -11 and -24
423 cm, and in the drained sites -28 and -41 cm during years 2011 and 2013, respectively,
424 (negative values indicate belowground WT). The two drained sites differed from each other,
425 so that D2 had shallower WT than D1 in both years (Fig. 1). During late summer 2013 all
426 sites experienced very low WT for an extended period (Fig. 1b).

427

428 Open top chambers (OTC) increased average air temperatures by 1.4°C compared to
429 ambient-T plots. The difference between OTC and Ambient-T plots was higher during spring
430 (1.8°C) and summer (1.6°C) than during autumn (0.5°C) (Table 1). Average soil
431 temperatures were not elevated by the OTCs (Table 1). Annual and summer average
432 temperatures were higher, and precipitation slightly higher, in years 2011 and 2013 than the
433 long term averages (Table 2).

434 **3.2. Leaf area index**

435 Land use had a clear impact on LMAX as it was lower in drained sites and at the comparable
436 level in restored and undrained sites (Fig. 2, Table S1.1.). Warming treatment increased
437 LMAX on average by 0.4 m²m⁻², and LMAX was lower in year 2013 than in 2011 (Fig.2,
438 Table S1.2.). The timing of the LMAX (LMAX_T) was dependent on land use and year
439 (Table S1.1.). LMAX was attained earlier in restored sites than in undrained sites and earlier
440 in year 2013 than in 2011 (Table S1.2.). The site groups 1 and 2 did not differ from each
441 other (Table S1.2.)

442 **3.3. Greenhouse Gas exchange**

443 **3.3.1. CO₂ exchange**

444 At the ambient-T plots, average field layer gross photosynthesis at full light (PPFD>800)
445 ranged from 537 to 1116 mg CO₂ m⁻² h⁻¹. In the warmed plots, the range was from 657 to
446 1122 mg CO₂ m⁻² h⁻¹. (Table 3). Average ecosystem respiration rates (Reco) ranged from 337
447 to 751 mg CO₂ m⁻² h⁻¹. In the warmed plots, the range was from 335 to 525 mg CO₂ m⁻² h⁻¹
448 (Table 3).

449

450 We based our CO₂ modelling on the relationship between NEE and PPFD, which is a strong
451 controller of photosynthesis (Fig. 3). The nonlinear mixed effect models showed that P_{MAX}
452 varied between land use categories; drained sites had lower P_{MAX} than undrained sites (Table
453 S2.2.). Experimental warming, as such, had no impact on P_{MAX}. (Table S2.1.) After inclusion
454 of environmental variables (i.e. the full model), the effect of land use was overridden by air
455 temperature and LAI implying that the treatment impact is dominated by changes in these
456 factors (Table S2.3. and S2.4.). The model indicated that drained sites had slightly higher
457 Reco than undrained sites, (Table S2.2.). As the- site group, i.e. group 1 with successful
458 drainage and group 2 with low drainage impact, was significant in the model, so that group 1
459 had higher Reco, the difference between properly drained site D1 and undrained sites is
460 stronger than indicated by the insignificant p-value (Table S2.2.). At the drained sites, the
461 respiration component includes tree root respiration but not respiration of the above-ground
462 parts of the trees, therefore the real Reco would be higher. The tree stand net primary
463 productivity is included in the estimate of seasonal NEE. Warming had no impact on Reco,
464 and Reco was higher in year 2013 than in 2011. In the full model, the environmental
465 variables air and soil temperature and LAI had a significant impact on Reco (Table S2.3.,
466 Table S2.4.). The maximum quantum yield of CO₂ assimilation (α), i.e., the light-use
467 efficiency at low light, was lower at drained sites and similar in restored and undrained sites
468 (Table S2.2., Table S2.4.).

469 The growing season cumulative NEE of the field layer and soil varied between -1088
470 (source) and +567 (sink) g CO₂ m⁻² season⁻¹. Unlike in undrained and restored sites, in the
471 drained sites the tree stand also sequestered carbon. The tree stand volumes were low, being
472 106 and 37 m³ ha⁻¹ in sites D1 and D2, respectively at year 2013. The average annual volume
473 increment since 2005 has been 5 and 2 m³ ha⁻¹ year⁻¹ representing annual carbon sequestration
474 of 959 and 423 g CO₂ m⁻² for sites D1 and D2, respectively. As most of the carbon
475 sequestration to the trees occurs during the growing season, we consider the annual value
476 comparable to our growing season field layer NEE estimate. At the more productive site, D1,
477 the NEE after inclusion of tree stand sequestration was about the same magnitude as in
478 undrained site, while site D2 was a strong CO₂ source (Fig. 4a). Generally, all the sites varied
479 from being small sources or sinks with clear inter annual variation. NEE was lower/negative
480 during dry year 2013 and higher under warming treatment than under ambient-T conditions
481 (Fig. 4a).

482

483 **3.3.2. Methane emissions**

484 The average measured CH₄ emissions varied between land use and warming treatments from
485 0.21 to 1.00 mg CH₄ m⁻² h⁻¹ (Table 3). The monthly variation in flux rates was rather large,
486 with highest fluxes in early summer and lower fluxes in late summer and autumn (Fig. 5).
487 Drained sites had somewhat lower emissions than undrained ones. Experimental warming
488 increased CH₄ flux in undrained sites, but not in restored and drained sites (Table S3.1, Table
489 S3.2.). When environmental variables were included in the model, the variation in CH₄ flux
490 was explained by water table and air temperature (Fig. 6, Table S3.3.), leaving LAI with
491 insignificant effect. Seasonal CH₄ emissions were lowest at drained sites (on average 0.2 g
492 CH₄ m⁻² season⁻¹) and highest at restored sites (on average 1.5 g CH₄ m⁻² season⁻¹) (Fig 4b).

493

494 **3.3.3. N₂O emissions**

495 The average measured N₂O emissions varied between treatments from 0.15 to 0.27 mg m⁻² h⁻¹
496 (Fig. 7, Table 3). Drained sites had higher emissions than undrained sites and warming
497 caused a slight but statistically insignificant increase on the emission, however, less in
498 drained sites than in other sites (Table S4.2.). None of the environmental variables included
499 in the model (WT, Ta, LAI) explained the variation in flux rates (Table S4.3.). The seasonal
500 N₂O emissions were lowest at undrained sites (on average 0.6 g N₂O m⁻² season⁻¹) and
501 highest at drained sites (on average 0.9 g N₂O m⁻² season⁻¹) (Fig 4c).

502 **3.3.4. Global warming potential**

503 At ambient-T conditions the GWP (CO₂ equivalent emissions) was positive, i.e., warming, at
504 most sites, and the drier year 2013 had higher GWP than 2011 (Table 4). The carbon
505 sequestration of tree stand at site D1 clearly decreased its GWP.

506 **4. Discussion**

507 Our experimental set-up with two references, namely the forestry drained starting point and
508 the undrained goal, allows the examination of a restoration pathway – is it going towards the
509 pristine conditions or to some new state? Our results show that restoration had led towards
510 pristine conditions by returning, within 3 years, the key ecosystem functions typical of
511 pristine mires. We found no differences in LAI or any gas flux components (P_{MAX}, Reco,
512 NEE, CH₄ or N₂O) between restored and undrained sites, while the long-term forestry
513 drainage had changed all these ecosystem functions. The response of the functions to
514 restoration had same direction but was faster than what was observed from deep peat
515 *Sphagnum* mires also drained for forestry (Kareksela et al. 2015).

516

517 **4.1. Field layer leaf area index**

518 At the forestry-drained state, which is the starting point for restoration, the LAI of field layer
519 vegetation was lower than at undrained state. This difference was mostly caused by a
520 decrease of sedge cover greater than the increase of shrub cover, indicating secondary
521 succession towards forest vegetation (the changes in species composition are shown at Laine
522 et al. 2016). During secondary succession following drainage, the closing tree canopy
523 increases the competition for light and decreases the biomass of field layer vegetation,
524 especially in minerotrophic mires (Laine et al. 1995; Minkkinen et al. 1999). In our study, no
525 longer than three years after restoration, LAI had already reached the range of undrained sites
526 and vegetation composition was shifting towards that of undrained sites (Laine et al. 2016).
527 We conclude that the largest share of the LAI change was due an increase in sedge cover
528 (Laine et al. 2016). Sedges are known to be the first species to respond to increased water
529 table level and light (Komulainen et al. 1999; Tuittila et al. 2000b; Graf et al. 2008).

530

531 OTC's installed at mires generally have rather modest impact on temperatures, with air
532 temperature increasing typically less than 2°C and soil temperatures less than 1°C (Turetsky
533 et al. 2008; Chivers et al. 2009; Johnson et al 2013; Munir, Strack 2014; Pearson et al. 2015;
534 Buttler et al 2015). Similarly, OTC's in our young primary mires increased the air
535 temperature less than 2°C, while soil temperature remained similar to the ambient-T plots.
536 The most evident effect of warming was the increased field layer LAI, which was observed in
537 all land use categories. This is in contrast to the study by Mäkiranta et al. (2017), who
538 observed no warming-induced changes in total leaf area in two sedge fens. The fast responses
539 of vascular plant LAI to warming at our sites may be due to the insignificant cover of

540 *Sphagnum* mosses, which are known to buffer plant community responses to environmental
541 manipulations (Wiedermann et al. 2007). Warming with OTCs has been shown to increase
542 vegetation height (Cornelius et al. 2014) and Normalized Difference Vegetation Index
543 (NDVI) (Buttler et al 2015), but the impacts on vegetation cover have been highly species-
544 specific (Buttler et al 2015). As an example, dwarf shrubs and graminoids have showed a
545 greater growth response to warming than herbaceous perennials (Kudernatsch et al., 2008).
546 On the other hand, we observed increased LAI under all land use types despite their
547 differences in plant community composition. According to a meta-analysis by Elmendorf et
548 al. (2012), in tundra there is large heterogeneity in the direction and magnitude of vegetation
549 responses, depending for example on the duration of warming experiment, ambient summer
550 temperatures, and moisture status.

551

552 Differences in LAI between the two measurement years of our study highlight the
553 responsiveness of primary mires to short-term water table drops. The summer 2013 drought
554 caused a clear decrease in LAI across the land use categories, despite similar average
555 temperatures to summer 2011.

556

557 **4.2. CO₂ exchange**

558 We found very high interannual and between site variability in the NEE of undrained sites
559 (ranging from -300 to 300 g CO₂ m⁻² season⁻¹). Such interannual variation is a typical
560 phenomenon in mires, and extreme drought can switch a mire into a CO₂ source (e.g. Alm et
561 al. 1999, Lund et al. 2012). When considering the wintertime CO₂ emission of ~130 g CO₂ m⁻²
562 season⁻¹ (estimated for the undrained sites at winter 2003/2004 by Leppälä et al. 2011b), the

563 annual uptake during year 2011 fits well within the range measured from temperate and
564 boreal mires (Roulet et al., 2007; Aurela et al. 2009; Christensen et al. 2012; McVeigh et
565 al. 2014; Peichl et al. 2014; Helfter et al. 2015), while during 2013 the NEE was clearly
566 lower.

567

568 Higher soil respiration rates are considered the main consequence of mire drainage, as
569 decomposition in well-aerated soil is many-fold more efficient than in anoxic conditions and
570 root respiration increases along with developing tree stands (e.g. Silvola et al. 1996;
571 Minkkinen et al. 2007; Maljanen et al. 2010; Chivers et al. 2017). In accordance, we observed
572 higher ecosystem respiration (excluding aboveground tree respiration) from the drained sites,
573 particularly from the successfully drained site D1 compared to undrained ones. In addition to
574 lower water table, the sites differ from each other in that drained sites have significant
575 amount of tree roots, which are lacking from undrained sites. Based on estimate from a
576 Finnish forestry drained mire, 10 to 20 % of the respiration may be produced by tree roots
577 (Minkkinen et al. 2018). In addition to increased respiration rates, drainage decreased the
578 photosynthetic capacity (P_{MAX}) of the field layer vegetation and shifted production to the
579 growing tree stand. The low P_{MAX} of field layer vegetation results from a combination of 1)
580 lower LAI, which is a proxy of the amount of photosynthetic tissue and therefore sets the
581 limit for photosynthesis (e.g. Barr et al. 2004; Wilson et al. 2007), and 2) the different species
582 composition due to differences in species photosynthetic capacities (e.g. Laine et al. 2016;
583 Korrensalo et al. 2016). When combined with lower light levels under the tree canopy, the
584 cumulative growing season NEE of field layer was clearly lower at the drained sites than at
585 the undrained sites, and was similar to a drained deep peat pine bog in Southern Finland
586 (Badorek et al. 2011). Including tree stand C sequestration, the well drained site D1 turned

587 into a small CO₂ sink during the less dry year, while the site D2 was a strong CO₂ source
588 during both years. In some forestry drained mires, the growth of the tree stand has exceeded
589 the C release from the decomposing peat, resulting in a large C sink (e.g. Lohila et al. 2011;
590 Ojanen et al. 2013; Hommeltenberg et al. 2014; Minkkinen et al. 2018; Ojanen et al.
591 unpublished data.). All such sites have been nutrient poor but still able to support intensive
592 tree growth. The tree growth in our site D2, on the other hand, was low due to poor drainage
593 and regular spring and autumn floods (Laine et al. 2016); this led to high CO₂ emissions.

594

595 Unlike in the drained sites, we did not find any differences in P_{MAX}, Reco and NEE
596 between restored and undrained sites. Indeed, decreased respiration rates are an expected
597 phenomena and a major goal of rewetting in mires (e.g. Waddington et al. 2010; Knox et al.
598 2015; Wilson et al. 2016).

599

600 In contrast to our hypothesis, experimental warming increased NEE, i.e. CO₂ sink capacity in
601 all land use types. The magnitude of the warming impact was, however, secondary to that of
602 land use induced water table alteration. Biochemical processes linked with photosynthesis are
603 controlled by temperature (e.g. Medlyn et al. 2002) and the importance of temperature in
604 controlling respiration in mires has been well documented (e.g. Lafleur et al. 2005; Mäkiranta
605 et al. 2009). Correspondingly, we found that both components of CO₂ exchange, P_{MAX} and
606 Reco, were dependent on air temperature. However, the impact of warming was seen only
607 after the instantaneous measured flux rates were reconstructed to cumulative growing season
608 fluxes. As OTC's were lifted up during the instantaneous measurements, they are made under
609 ambient temperature conditions, which are similar at both OTC and ambient-T plots and not
610 influenced by the OTC warming except via the indirect effect of increased leaf area. In

611 several other studies moderate warming has had very small or no impact on CO₂ fluxes
612 (Chivers et al. 2009; Johnson et al. 2013; Pearson et al. 2015), while some have reported a
613 moderate increase in respiration (Ward et al. 2013). Voigt et al. (2017) observed clear
614 decrease in NEE, as, in addition to increased ecosystem respiration, plants were suffering
615 from increased water deficient due to warming. Ward et al. (2013) noticed that the response
616 was dependent on the existing plant groups so that NEE increased only when graminoids
617 were removed, leaving only shrubs and mosses. In our sites, plants seemed to be able to
618 respond to warming by increasing leaf area and photosynthesis and we observed quite similar
619 increases in cumulative NEE due to warming in shrub-dominated drained sites and
620 graminoid-dominated undrained and restored sites.

621

622 **4.3.Methane emissions**

623 Methane emissions were at the low end of those measured from different fens (e.g. Suyker et
624 al. 1996; Rinne et al. 2007; Nilsson et al. 2008; Leppälä et al. 2011c; Trudeau et al. 2013).
625 Similar to previous findings, CH₄ emissions were controlled by water table and air
626 temperature (e.g. Moore, Dalva 1993; Bubier et al. 1993; Pelletier et al. 2007; Lai 2009).
627 Water table and air temperature overruled any effects of LAI in explaining the CH₄
628 emissions, even though vegetation functions as a supply of organic material for methanogens
629 and as a pathway of methane through the aerobic peat layer (Ström et al. 2003; Garnet et al.
630 2005).

631

632 While the literature shows that drainage decreases or ceases CH₄ emissions (Martikainen et
633 al. 1995; Roulet, Moore 1995; Maljanen et al. 2010; Frohking et al. 2011), we found only
634 slightly lower CH₄ emissions from drained sites compared to undrained ones. This small

635 difference is likely a result of the low water table throughout most of the studied growing
636 seasons at all sites. When comparing our measurements with previous study from the same
637 undrained sites it is evident that the low water table had decreased the CH₄ fluxes: during a
638 wet year (2004), the seasonal cumulative CH₄ emission was much higher than during our
639 measurement years (8.8 compared to 0.8 g CH₄ m⁻² season⁻¹; Fig. 4b, Leppälä et al. 2011c).
640 Mire restoration is often associated with highly increased methane emission, although there is
641 a large range of emissions (0-91 g CH₄ m⁻² yr⁻¹) between the studies, caused by differences in
642 water table, vegetation composition and time since restoration (Knox et al. 2014; Nahlik,
643 Mitsch, 2010; Hendriks et al. 2007; Herbst et al., 2013; Wilson et al. 2016). We assume that
644 during wetter years CH₄ emissions at the restored sites would be similar to those that have
645 been measured from these undrained sites (Leppälä et al 2011c). This is supported by
646 similarities in the vegetation composition and WT dynamics between our undrained and
647 restored sites. In addition, there are indications that at our sites the soil microbial community,
648 both methanogens and methanotrophs, was recovering rapidly after restoration (Putkinen et
649 al. 2012).

650

651 Warming increased CH₄ fluxes, but only at the undrained sites. Both microbial methane
652 production and oxidation are dependent on temperature (Dunfield et al. 1993), and the
653 existing studies on warming impacts are inconclusive. Turetsky et al. (2008) found increased
654 and Peltoniemi et al. (2016) decreased methane emissions in fens, while some other studies
655 have found no impact (Johnson et al. 2013; Pearson et al. 2015). The warming impact is
656 likely dependent on moisture conditions as in water-saturated conditions emissions have
657 increased, while the opposite has been observed from drier hummocks (Munir, Strack 2014;
658 Gill et al. 2017). This is partly in accordance with our study, as the water table was generally
659 higher in undrained than in drained sites. Why CH₄ fluxes at the restored sites did not

660 respond similarly to warming remains an unanswered question, however, as the restored and
661 undrained water tables were similar, and Putkinen et al. (2012) showed that the methanogen
662 community was not poorly developed and therefore would be able to respond to warming.

663

664 **4.4. Nitrous oxide**

665 Nitrous oxide plays a minor role in the GHG dynamics of these primary mires. We measured
666 higher N₂O fluxes from drained sites than from undrained sites, which is typical especially in
667 fen mires (Regina et al. 1996; Ojanen et al. 2010; Pearson et al. 2015). The flux rates were
668 within the range measured from other Finnish forestry drained mires (Ojanen et al. 2010). We
669 observed modest seasonal variability in the flux rates and were not able to explain the fluxes
670 with environmental variables, although temperate and moisture conditions are generally seen
671 as regulators of seasonal flux variability (Kitzler et al. 2006). The experimental warming
672 seemed to increase the N₂O fluxes, likely due to high temperature sensitivity of
673 denitrification and consequently N₂O fluxes (Butterbach-Bahl et al. 2013). Our finding is in
674 contrast to earlier studies from pristine mires (Ward et al. 2013, Pearson et al. 2015), but the
675 disparity may be explained by differences in moisture conditions and other site characteristics
676 as they may restrain the stimulating effect of temperature (Butterbach-Bahl, Dannenmann
677 2011). Our data set on N₂O is however, limited to five measurement campaigns, and do to a
678 sporadic nature of N₂O emissions (Butterbach-Bahl et al. 2013) we would not draw any
679 strong conclusions from this result.

680

681 **5. Conclusions**

682 In our study, restoration appeared to be an effective climate mitigation tool; restoration
683 quickly returned the ecosystem functions of undrained primary mires and reversed unwanted

684 impacts of drainage, such as high respiration rates. The global warming potential (GWP)
685 varied largely between sites and years, and most sites, including the undrained ones, had a
686 positive GWP, especially during the dry year 2013. It seems that restoration of boreal forestry
687 drained mires is relatively fast and easy task compared to mires drained for agricultural
688 purposes (Klimkowska et al. 2007) or peat harvesting areas (Chimner et al. 2017). A likely
689 reason is that forestry drainage causes less disturbance to vegetation cover and soil. These
690 differences should be further evaluated. In restored, as well as other sites, warming
691 accelerated net ecosystem CO₂ sink function, due to increased LAI and we did not see any
692 signs that moderate warming would compromise the climate mitigation of restoration.

693

694 **Acknowledgements**

695 We acknowledge funding from the University of Helsinki and Kone foundation (A. M.
696 Laine), the Natural Resources Institute Finland (A. Tolvanen), the Fulbright-Finland and
697 Saastamoinen Foundations (S. Froking), and the Academy of Finland (project code 287039)
698 (E.-S. Tuittila). We thank Ivka Vasil`ka, Annukka Närhi and Mirikka Kotiaho for field
699 assistance.

700 **Data Statement**

701 The datasets generated during and/or analysed during the current study are available from the
702 corresponding author on request.

703 **Supplementary material for online publication:**

704 **Supporting information 1. Nonlinear mixed-effect model based on leaf area index**

705 **Supporting information 2. Nonlinear mixed-effect model based on CO₂ flux**
706 **measurements**

707 **Supporting information 3. Linear mixed effect models based on CH₄ measurements**

708 **Supporting information 4. Linear mixed effect models based on N₂O measurements**

709

710

711 References

- 712 Aichi Biodiversity Targets. 2011. Convention on Biological Diversity, 2011. Strategic Plan
713 for Biodiversity 2011–2020. Available at <http://www.cbd.int/sp/targets/>. (accessed 16th
714 January 2018).
- 715 Alm, J., Schulman, L., Walden, J., Nykänen, H., Martikainen, P. J. Silvola, J., 1999. Carbon
716 balance of a boreal bog during a year with an exceptionally dry summer. *Ecology* 80, 161–
717 174.
- 718 Alm, J., Shurpali, N. J., Tuittila, E. S., Laurila, T., Maljanen, M., Saarnio, S., Minkkinen, K.,
719 2007. Methods for determining emission factors for the use of peat and peatlands flux
720 measurements and modelling. *Boreal Environ. Res.* 12, 85–100.
- 721 Aurela, M., Lohila, A., Tuovinen, J. P., Hatakka, J., Riutta, T., Laurila, T., 2009. Carbon
722 dioxide exchange on a northern boreal fen. *Boreal Environ. Res.* 14, 699-710.
- 723 Badorek, T., Tuittila, E. S., Ojanen, P., Minkkinen, K., 2011. Forest floor photosynthesis and
724 respiration in a drained peatland forest in southern Finland. *Plant Ecology, Diversity* 4(2-3),
725 227-241.
- 726 Barr, A. G., Black, T. A., Hogg, E. H., Kljun, N., Morgenstern, K., Nesic, Z., 2004. Inter-
727 annual variability in the leaf area index of a boreal aspen-hazelnut forest in relation to net
728 ecosystem production. *Agricultural and Forest Meteorology* 126(3), 237-255.
- 729 Bonn, A., Reed, M. S., Evans, C. D., Joosten, H., Bain, C., Farmer, J., Emmer, I.,
730 Couwenberg, J., Moxey, A., Artz, R., Tanneberger, F., von Unger, M., Smyth, M.-A., Birnie,
731 D., 2014. Investing in nature, developing ecosystem service markets for peatland restoration.
732 *Ecosystem Services* 9, 54-65.

733 Bubier, J. L., Moore, T. R., Roulet, N. T., 1993. Methane emissions from wetlands in the
734 midboreal region of northern Ontario, Canada. *Ecology* 74(8), 2240-2254.

735 Butterbach-Bahl, K., Dannenmann, M., 2011. Denitrification and associated soil N₂O
736 emissions due to agricultural activities in a changing climate. *Current Opinion in*
737 *Environmental Sustainability* 3(5), 389-395.

738 Butterbach-Bahl, K., Baggs, E. M., Dannenmann, M., Kiese, R., Zechmeister-Boltenstern, S.,
739 2013. Nitrous oxide emissions from soils: how well do we understand the processes and their
740 controls?. *Phil. Trans. R. Soc. B.* 368(1621), 20130122.

741 Buttler, A., Robroek, B. J.M., Laggoun-Défarge, F., Jassey, V. E.J., Pochelon, C., Bernard,
742 G., Delarue, F., Gogo, S., Mariotte, P., Mitchell, E. A.D. Bragazza, L., 2015. Experimental
743 warming interacts with soil moisture to discriminate plant responses in an ombrotrophic
744 peatland. *Journal of Vegetation Science* 26, 964–974.

745 Chimner, R. A., Cooper, D. J., Wurster, F. C., Rochefort, L., 2017. An overview of peatland
746 restoration in North America: where are we after 25 years?. *Restoration Ecology* 25(2), 283-
747 292.

748 Chivers, M. R., Turetsky, M. R., Waddington, J. M., Harden, J. W., McGuire, A. D., 2009.
749 Effects of experimental water table and temperature manipulations on ecosystem CO₂ fluxes
750 in an Alaskan rich fen. *Ecosystems* 12(8), 1329-1342.

751 Christensen, T. R., Jackowicz-Korczyński, M., Aurela, M., Crill, P., Heliasz, M.,
752 Mastepanov, M., Friborg, T., 2012. Monitoring the multi-year carbon balance of a subarctic
753 palsamire with micrometeorological techniques. *Ambio* 41(3), 207-217.

754 Cornelius, C., Heinichen, J., Drösler, M., Menzel, A., 2014. Impacts of temperature and water
755 table manipulation on grassland phenology. *Applied Vegetation Science* 17(4), 625-635.

756 Dorrepaal, E., Toet, S., van Logtestijn, R. S., Swart, E., van de Weg, M. J., Callaghan, T. V.,
757 Aerts, R., 2009. Carbon respiration from subsurface peat accelerated by climate warming in
758 the subarctic. *Nature* 460(7255), 616-619.

759 Dunfield, P., Dumont, R., Moore, T. R., 1993. Methane production and consumption in
760 temperate and subarctic peat soils, response to temperature and pH. *Soil Biology and*
761 *Biochemistry* 25(3), 321-326.

762 Ekman, M., 1996. A consistent map of the postglacial uplift of Fennoscandia. *Terra Nova*
763 8(2), 158-165.

764 Elmendorf, S. C., Henry, G. H. R., Hollister, R. D., Björk, R. G., Bjorkman, A. D.,
765 Callaghan, T. V., Collier, L. S., Cooper, E. J., Cornelissen, J. H. C., Day, T. A., Fosaa, A. M.,
766 Gould, W. A., Grétarsdóttir, J., Harte, J., Hermanutz, L., Hik, D. S., Hofgaard, A., Jarrad, F.,
767 Jónsdóttir, I. S., Keuper, F., Klanderud, K., Klein, J. A., Koh, S., Kudo, G., Lang, S. I.,
768 Loewen, V., May, J. L., Mercado, J., Michelsen, A., Molau, U., Myers-Smith, I. H.,
769 Oberbauer, S. F., Pieper, S., Post, E., Rixen, C., Robinson, C. H., Schmidt, N. M., Shaver, G.
770 R., Stenström, A., Tolvanen, A., Totland, Ø., Troxler, T., Wahren, C.-H., Webber, P. J.,
771 Welker, J. M., Wookey, P. A., 2012, Global assessment of experimental climate warming on
772 tundra vegetation: heterogeneity over space and time. *Ecology Letters* 15: 164–175.

773 EU Biodiversity Strategy to 2020, European Commission, 2012. EU Biodiversity Strategy to
774 2020. Available at [http:// ec.europa.eu/environment/nature/biodiversity/comm2006/
775 2020.htm](http://ec.europa.eu/environment/nature/biodiversity/comm2006/2020.htm). (accessed 16 January 2018).

776 Frohking, S., Roulet, N. T., 2007. Holocene radiative forcing impact of northern peatland
777 carbon accumulation and methane emissions. *Global Change Biology* 13(5), 1079-1088.

778 Frohking, S., Talbot, J., Jones, M. C., Treat, C. C., Kauffman, J. B., Tuittila, E. S., Roulet, N.,
779 2011. Peatlands in the Earth's 21st century climate system. *Environ. Rev.* 19, 371-396.

780 Garnet, K. N., Megonigal, J. P., Litchfield, C., Taylor, G. E., 2005. Physiological control of
781 leaf methane emission from wetland plants. *Aquatic Botany* 81(2), 141-155.

782 Gill, A. L., Giasson, M. A., Yu, R., Finzi, A. C., 2017. Deep peat warming increases surface
783 methane and carbon dioxide emissions in a black spruce dominated ombrotrophic bog.
784 *Global Change Biology* 23: 5398-5411.

785 Graf, M. D., Rochefort, L., Poulin, M., 2008. Spontaneous revegetation of cutaway
786 peatlands of North America. *Wetlands* 28(1), 28-39.

787 Harrell Jr, F. E., 2001. Regression modeling strategies, with applications to linear models,
788 logistic and ordinal regression, and survival analysis. Springer New York.

789 Heinonen, J., 1994. KPL-koealojen puu- ja puustotunnusten laskentaohjelman käyttöohje. (A
790 guide to calculate tree- and treestand parameters of KPL-sample plots.) (in Finnish). The
791 Finnish Forest Research Institute Research Papers 504, 1–80.

792 Helfter, C., Campbell, C., Dinsmore, K. J., Drewer, J., Coyle, M., Anderson, M., Skiba, U.,
793 Nemitz, E., Billett, M. F., Sutton, M. A., 2015. Drivers of long-term variability in CO₂ net
794 ecosystem exchange in a temperate peatland. *Biogeosciences* 12(6), 1799-1811.

795 Hellemaa, P., 1998. The development of coastal dunes and their vegetation in Finland. *Fennia*
796 - *International Journal of Geography* 176, 111-221.

797 Hendriks, D. M. D., Van Huissteden, J., Dolman, A. J., Van der Molen, M. K., 2007. The full
798 greenhouse gas balance of an abandoned peat meadow. *Biogeosciences Discussions* 4(1),
799 277-316.

800 Herbst, M., Friborg, T., Schelde, K., Jensen, R., Ringgaard, R., Vasquez, V., Thomsen, A. G.,
801 Søgaard, H., 2013. Climate and site management as driving factors for the atmospheric
802 greenhouse gas exchange of a restored wetland. *Biogeosciences* 10(1), 39-52.

803 Hobbs, R. J., Cramer, V. A., 2008. Restoration ecology: interventionist approaches for
804 restoring and maintaining ecosystem function in the face of rapid environmental change.
805 *Annu. Rev. Environ. Resour.* 33, 39–61.

806 Hommeltenberg, J., Schmid, H. P., Drösler, M., Werle, P., 2014. Can a bog drained for
807 forestry be a stronger carbon sink than a natural bog forest?. *Biogeosciences* 11(13), 3477-
808 3493.

809 Intergovernmental Panel on Climate Change (IPCC), 2013. *Climate Change 2013: The*
810 *Physical Science Basis. Contribution of Working Group I to the Fifth Assessment Report of*
811 *the Intergovernmental Panel on Climate Change* [Stocker, T.F., D. Qin, G.-K. Plattner, M.
812 Tignor, S.K. Allen, J. Boschung, A. Nauels, Y. Xia, V. Bex, P.M. Midgley (eds.)].
813 Cambridge University Press, Cambridge, United Kingdom and New York, NY, USA.

814 Jauhiainen, J., Page, S. E., Vasander, H., 2016. Greenhouse gas dynamics in degraded and
815 restored tropical peatlands. *Mires and Peat* 17, 1–12.

816 Johnson, C. P., Pypker, T. G., Hribljan, J. A., Chimner, R. A., 2013. Open top chambers and
817 infrared lamps, A comparison of heating efficacy and CO₂/CH₄ dynamics in a northern
818 Michigan peatland. *Ecosystems* 16(5), 736-748.

819 Joosten, H., Tannenberger, F., Moen, A. 2017. *Mires and peatlands of Europe..*
820 Schweizerbart Science Publishers, Stuttgart, Germany, p. 780.

821 Joosten, H., 2010. The global peatland CO₂ picture: peatland status and drainage related
822 emissions in all countries in the world. Report for Wetlands International, Wageningen, The
823 Netherlands.

824 Kareksela, S., Haapalehto, T., Juutinen, R., Matilainen, R., Tahvanainen, T., Kotiaho, J. S.,
825 2015. Fighting carbon loss of degraded peatlands by jump-starting ecosystem functioning
826 with ecological restoration. *Science of the Total Environment* 537, 268-276.

827 Kitzler, B., Zechmeister-Boltenstern, S., Holtermann, C., Skiba, U., Butterbach-Bahl, K.,
828 2006. Nitrogen oxides emission from two beech forests subjected to different nitrogen loads.
829 *Biogeosciences* 3(3), 293-310.

830 Klimkowska, A., Van Diggelen, R., Bakker, J. P., Grootjans, A. P., 2007. Wet meadow
831 restoration in Western Europe: a quantitative assessment of the effectiveness of several
832 techniques. *Biological Conservation* 140(3-4), 318-328.

833 Knox, S. H., Sturtevant, C., Matthes, J. H., Koteen, L., Verfaillie, J., aldocchi, D., 2015.
834 Agricultural peatland restoration, effects of land-use change on greenhouse gas (CO₂ and
835 CH₄) fluxes in the Sacramento-San Joaquin Delta. *Global Change Biology* 21(2), 750-765.

836 Komulainen, V. M., Nykänen, H., Martikainen, P. J., Laine, J., 1998. Short-term effect of
837 restoration on vegetation change and methane emissions from peatlands drained for forestry
838 in southern Finland. *Canadian Journal of Forest Research* 28(3), 402-411

839 Komulainen, V. M., Tuittila, E. S., Vasander, H., Laine, J., 1999. Restoration of drained
840 peatlands in southern Finland, initial effects on vegetation change and CO₂ balance. *Journal*
841 *of Applied Ecology* 36(5), 634-648.

842 Korrensalo, A., Hájek, T., Vesala, T., Mehtätalo, L., Tuittila, E. S., 2016. Variation in
843 photosynthetic properties among bog plants. *Botany* 94(12), 1127-1139.

844 Koskinen, M., Maanavilja, L., Nieminen, M., Minkkinen, K., Tuittila, E. S., 2016. High
845 methane emissions from restored Norway spruce swamps in southern Finland over one
846 growing season. *Mires and Peat* 17, 1-13.

847 Kudernatsch, T., Fischer, A., Bernhardt-Römermann, M., Abs, C., 2008. Short-term effects of
848 temperature enhancement on growth and reproduction of alpine grassland species. *Basic and*
849 *Applied Ecology* 9(3), 263-274.

850 Lafleur, P. M., Moore, T. R., Roulet, N. T., Frolking, S., 2005. Ecosystem respiration in a
851 cool temperate bog depends on peat temperature but not water table. *Ecosystems* 8(6), 619-
852 629.

853 Lai, D. Y. F., 2009. Methane dynamics in northern peatlands, a review. *Pedosphere* 19(4),
854 409-421.

855 Laiho, R., Laine, J., 1997. Tree stand biomass and carbon content in an age sequence of
856 drained pine mires in southern Finland. *Forest Ecology and Management* 93(1-2), 161-169.

857 Laine, A. M., Tolvanen, A., Mehtätalo, L., Tuittila, E. S., 2016. Vegetation structure and
858 photosynthesis respond rapidly to restoration in young coastal fens. *Ecology and Evolution*,
859 6(19), 6880-6891.

860 Laine, J., Vasander, H., Laiho, R., 1995. Long-term effects of water level drawdown on the
861 vegetation of drained pine mires in southern Finland. *Journal of Applied Ecology* 32, 785-
862 802.

863 Laitinen, J., Rehell, S., Oksanen, J., 2008. Community and species responses to water level
864 fluctuations with reference to soil layers in different habitats of mid-boreal mire complexes.
865 *Plant Ecology* 194(1), 17-36.

866 Lappi, J., Oker-Blom, P. 1992. Characterizing photosynthetic radiation response or other
867 output function as a mean of element responses. *J. Theor. Biol.* 154, 371–389.

868 Leppälä, M., Laine, A. M., Seväkivi, M. L., Tuittila, E. S., 2011a. Differences in CO₂
869 dynamics between successional mire plant communities during wet and dry summers. *Journal*
870 *of Vegetation Science* 22(2), 357-366.

871 Leppälä, M., Laine, A., Tuittila, E. S., 2011b. Winter carbon losses from a boreal mire
872 succession sequence follow summertime patterns in carbon dynamics. *Suo* 62(1), 1-11.

873 Leppälä, M., Oksanen, J., Tuittila, E. S., 2011c. Methane flux dynamics during mire
874 succession. *Oecologia* 165(2), 489-499.

875 Lohila, A., Minkkinen, K., Aurela, M., Tuovinen, J. P., Penttilä, T., Ojanen, P., Laurila, T.,
876 2011. Greenhouse gas flux measurements in a forestry-drained peatland indicate a large
877 carbon sink. *Biogeosciences* 8(11), 3203-3218.

878 Lund, M., Christensen, T. R., Lindroth, A., Schubert, P., 2012. Effects of drought conditions
879 on the carbon dioxide dynamics in a temperate peatland. *Environmental Research Letters*
880 7(4), 045704.

881 Lund, M., Lafleur, P. M., Roulet, N. T., Lindroth, A., Christensen, T. R., Aurela, M.,
882 Chojnicki, B. H., Flanagan, L. B., Humphreys, E. R., Laurila, T., Oechel, W. C., Olejnik, J.,
883 Rinne, J., Schubert, P., Nilsson, M. B., 2010. Variability in exchange of CO₂ across 12
884 northern peatland and tundra sites. *Global Change Biology* 16(9), 2436-2448.

885 Luoma, S., 1997. Geographical pattern in photosynthetic light response of *Pinus sylvestris* in
886 Europe. *Functional Ecology* 11(3), 273-281.

887 Maljanen, M., Sigurdsson, B. D., Guðmundsson, J., Óskarsson, H., Huttunen, J. T.,
888 Martikainen, P. J., 2010. Greenhouse gas balances of managed peatlands in the Nordic
889 countries—present knowledge and gaps. *Biogeosciences* 7(9), 2711-2738.

890 Martikainen, P. J., Nykänen, H., Alm, J., Silvola, J., 1995. Change in fluxes of carbon
891 dioxide, methane and nitrous oxide due to forest drainage of mire sites of different trophic. In
892 *Nutrient Uptake and Cycling in Forest Ecosystems* (pp. 571-577). Springer Netherlands.

893 McVeigh, P., Sottocornola, M., Foley, N., Leahy, P., Kiely, G., 2014. Meteorological and
894 functional response partitioning to explain interannual variability of CO₂ exchange at an Irish
895 Atlantic blanket bog. *Agricultural and Forest Meteorology* 194, 8-19.

896 Medlyn, B. E., Dreyer, E., Ellsworth, D., Forstreuter, M., Harley, P. C., Kirschbaum, M. U.
897 F., Le Roux, X., Montpied, P., Strassmeyer, J., Walcroft, A., Wang, K. Loustau, D., 2002.
898 Temperature response of parameters of a biochemically based model of photosynthesis. II. A
899 review of experimental data. *Plant, Cell, Environment* 25(9), 1167-1179.

900 Meng, L., Roulet, N., Zhuang, Q., Christensen, T. R., Frohking, S., 2016. Focus on the impact
901 of climate change on wetland ecosystems and carbon dynamics. *Environmental Research*
902 *Letters* 11(10), 100201.

903 Merilä, P., Galand, P. E., Fritze, H., Tuittila, E. S., Kukko-oja, K., Laine J., Yrjälä K., 2006.
904 Methanogen communities along a primary succession transect of mire ecosystems. *FEMS*
905 *Microbiol. Ecol.* 55, 221-229.

906 Miettinen, J., Shi, C., Liew, S. C., 2016. Land cover distribution in the peatlands of
907 Peninsular Malaysia, Sumatra and Borneo in 2015 with changes since 1990. *Global Ecology*
908 *and Conservation* 6, 67-78.

909 Minkkinen, K., Ojanen, P., Penttilä, T., Aurela, M., Laurila, T., Tuovinen, J.-P., Lohila, A.,
910 (2018, in review). Carbon accumulation in a drained boreal bog was decreased but not
911 stopped by seasonal drought, *Biogeosciences Discuss.*, <https://doi.org/10.5194/bg-2017-530>.

912 Minkkinen, K., Laine, J., Shurpali, N. J., Mäkiranta, P., Alm, J., Penttilä, T., 2007.
913 Heterotrophic soil respiration in forestry-drained peatlands. *Boreal Environmental Research*
914 12, 115–126

915 Minkkinen, K., Vasander, H., Jauhainen, S., Karsisto, M., Laine, J., 1999. Post-drainage
916 changes in vegetation composition and carbon balance in Lakkasuo mire, Central Finland.
917 *Plant and Soil* 207(1), 107-120.

918 Moore, T. R., Dalva, M., 1993. The influence of temperature and water table position on
919 carbon dioxide and methane emissions from laboratory columns of peatland soils. *Journal of*
920 *Soil Science* 44(4), 651-664.

921 Munir, T. M., Strack, M., 2014. Methane flux influenced by experimental water table
922 drawdown and soil warming in a dry boreal continental bog. *Ecosystems* 17(7), 1271-1285

923 Myhre, G., D. Shindell, F.-M. Bréon, W., Collins, J., Fuglestvedt, J., Huang, D., Koch, J.-F.
924 Lamarque, D., Lee, B., Mendoza, T., Nakajima, A., Robock, G., Stephens, T. Takemura, H.

925 Zhang., 2013. Anthropogenic and Natural Radiative Forcing. In: Climate Change 2013: The
926 Physical Science Basis. Stocker, T.F., D. Qin, G.-K. Plattner, M., Tignor, S.K., Allen, J.,
927 Boschung, A., Nauels, Y., Xia, V. Bex and P.M. Midgley (eds.), Contribution of Working
928 Group I to the Fifth Assessment Report of the Intergovernmental Panel on Climate Change.
929 Cambridge University Press Cambridge, United Kingdom and New York, NY, USA

930 Mäkiranta, P., Laiho, R., Fritze, H., Hytönen, J., Laine, J., Minkkinen, K., 2009. Indirect
931 regulation of heterotrophic peat soil respiration by water level via microbial community
932 structure and temperature sensitivity. *Soil Biology and Biochemistry* 41(4), 695-703.

933 Mäkiranta, P., Laiho, R., Mehtätalo, L., Straková, P., Sormunen, J., Minkkinen, K., Penttilä,
934 T., Fritze, H., Tuittila, E.-S., 2018. Responses of phenology and biomass production of boreal
935 fens to climate warming under different water-table level regimes. *Global Change Biology*
936 24, 944-956.

937 Mälson, K., Backéus, I., Rydin, H., 2007. Long-term effects of drainage and initial effects of
938 hydrological restoration on rich fen vegetation. *Applied Vegetation Science* 11(1), 99-106.

939 Nahlik, A. M., Mitsch, W. J., 2010. Methane emissions from created riverine wetlands.
940 *Wetlands* 30(4), 783-793.

941 Nilsson, M., Sagerfors, J., Buffam, I., Laudon, H., Eriksson, T., Grelle, A., Klemedtsson, L.,
942 Weslien, P., Lindroth, A., 2008, Contemporary carbon accumulation in a boreal oligotrophic
943 minerogenic mire – a significant sink after accounting for all C-fluxes. *Global Change*
944 *Biology* 14, 2317–2332.

945 Ojanen, P., Minkkinen, K., Penttilä, T., 2013. The current greenhouse gas impact of forestry-
946 drained boreal peatlands. *Forest Ecology and Management* 289, 201-208.

947 Ojanen, P., Minkkinen, K., Alm, J., Penttilä, T., 2010. Soil–atmosphere CO₂, CH₄ and N₂O
948 fluxes in boreal forestry-drained peatlands. *Forest Ecology and Management* 260(3), 411-
949 421.

950 Paavilainen, E., Päivänen, J., 1995. Peatland forestry, ecology and principles (Vol. 111) (250
951 pp). Springer Science, Business Media.

952 Parviainen, T., 1999. Sekametsikön koivujen biomassan ja latvusrakenteen selvittäminen
953 elintoimintoihin perustuvia kasvumalleja varten (Determining birch biomass and crown
954 structure in mixed forests to be used with growth models based in vital functions), MSc
955 Thesis. Department of Forest Ecology, University of Helsinki, Finland. (in Finnish.)

956 Pearson, M., Penttilä, T., Harjunpää, L., Laiho, R., Laine, J., Sarjala, T., Silvan, K., Silvan, N.,
957 2015. Effects of temperature rise and water-table-level drawdown on greenhouse gas fluxes
958 of boreal sedge fens. *Boreal Environment Research* 20(4), 489–505.

959 Peichl, M., Öquist, M., Löfvenius, M. O., Ilstedt, U., Sagerfors, J., Grelle, A., Lindroth,
960 A., Nilsson, M. B., 2014. A 12-year record reveals pre-growing season temperature and water
961 table level threshold effects on the net carbon dioxide exchange in a boreal fen.
962 *Environmental Research Letters* 9(5), 055006.

963 Pelletier, L., Moore, T. R., Roulet, N. T., Garneau, M., Beaulieu-Audy, V., 2007. Methane
964 fluxes from three peatlands in the La Grande Riviere watershed, James Bay lowland, Canada.
965 *Journal of Geophysical Research, Biogeosciences* 112(G1).

966 Peltoniemi, K., Laiho, R., Juottonen, H., Bodrossy, L., Kell, D. K., Minkkinen, K.,
967 Mäkiranta, P., Mehtätalo, L., Penttilä, T., Siljanen, H. M.P., Tuittila, E. S. Tuomivirta, T.,
968 Fritze, H., 2016. Responses of methanogenic and methanotrophic communities to warming in
969 varying moisture regimes of two boreal fens. *Soil Biology and Biochemistry* 97, 144-156.

970 Pinheiro, J. C., Bates D. M., 2000. Mixed-effects models in S and S-plus. Springer-Verlag,
971 New York.

972 Pirinen, P., Simola, H., Aalto, J., Kaukoranta, J. P., Karlsson, P., Ruuhela, R., 2012. Tilastoja
973 suomen ilmastosta 1981-2010. (Climatological statistics of Finland 1981-2010). (in Finnish),
974 Ilmatieteen laitos (Finnish Meteorological Institute), Helsinki.

975 Putkinen, A., Juottonen, H., Tuittila, E.-S., Peltoniemi, K., Tolvanen, A., Tuomivirta, T.,
976 Yrjälä, K., Fritze, H., 2012. Methane turnover before and after restoration of young forestry-
977 drained fens. In, Magnusson, T (ed.) Peatlands in Balance Book of Abstracts of the 14th
978 International Peat Congress.

979 Regina, K., Nykänen, H., Silvola, J., Martikainen, P. J., 1996. Fluxes of nitrous oxide from
980 boreal peatlands as affected by peatland type, water table level and nitrification capacity.
981 *Biogeochemistry* 35(3), 401-418.

982 Renou-Wilson, F., Barry, C., Müller, C., Wilson, D., 2014. The impacts of drainage, nutrient
983 status and management practice on the full carbon balance of grasslands on organic soils in a
984 maritime temperate zone. *Biogeosciences* 11(16), 4361-4379.

985 Repola, J., 2008. Biomass equations for birch in Finland. *Silva Fennica* 42(4), 605-624.

986 Repola, J. 2009. Biomass equations for Scots pine and Norway spruce in Finland. *Silva*
987 *Fennica* 43(4), 625-647.

988 Rinne, J., Riutta, T., Pihlatie, M., Aurela, M., Haapanala, S., Tuovinen, J. P., Tuittila, E.-S.,
989 Vesala, T., 2007. Annual cycle of methane emission from a boreal fen measured by the eddy
990 covariance technique. *Tellus B* 59(3), 449-457.

991 Roulet, N. T., Moore, T. R., 1995. The effect of forestry drainage practices on the emission of
992 methane from northern peatlands. *Canadian Journal of Forest Research* 25(3), 491-499.

993 Roulet, N. T., Lafleur, P. M., Richard, P. J., Moore, T. R., Humphreys, E. R., Bubier, J.,
994 2007. Contemporary carbon balance and late Holocene carbon accumulation in a northern
995 peatland. *Global Change Biology* 13(2), 397-411.

996 Silvola, J., Alm, J., Ahlholm, U., Nykanen, H., Martikainen, P. J., 1996. CO₂ fluxes from peat
997 in boreal mires under varying temperature and moisture conditions. *Journal of Ecology* 84,
998 219-228.

999 Strack, M., Zuback, Y. C. A., 2013. Annual carbon balance of a peatland 10 yr following
1000 restoration. *Biogeosciences* 10(5), 2885-2896.

1001 Ström, L., Ekberg, A., Mastepanov, M., Christensen, R. T., 2003. The effect of vascular
1002 plants on carbon turnover and methane emissions from a tundra wetland. *Global Change*
1003 *Biology* 9(8), 1185-1192.

1004 Suyker, A. E., Verma, S. B., Clement, R. J., Billesbach, D. P., 1996. Methane flux in a boreal
1005 fen, Season-long measurement by eddy correlation. *Journal of Geophysical Research,*
1006 *Atmospheres* 101(D22), 28637-28647.

1007 Tarvainen, O., Laine, A. M., Peltonen, M., Tolvanen, A., 2013. Mineralization and
1008 decomposition rates in restored pine fens. *Restoration Ecology* 21(5), 592-599.

1009 Trudeau, N. C., Garneau, M., Pelletier, L., 2013. Methane fluxes from a patterned fen of the
1010 northeastern part of the La Grande river watershed, James Bay, Canada. *Biogeochemistry*
1011 113(1-3), 409-422.

1012 Tuittila E.-S., Juutinen S., Froelking S., Väiliranta M., Laine A., Miettinen A., Quillet A.,
1013 Merilä P., 2013. Wetland chronosequence as a model of peatland development: Vegetation
1014 succession, peat and carbon accumulation. *The Holocene* 23: 23–33.

1015 Tuittila, E. S., Komulainen, V. M., Vasander, H., Laine, J., 1999. Restored cut-away peatland
1016 as a sink for atmospheric CO₂. *Oecologia* 120(4), 563-574.

1017 Tuittila, E.-S., Komulainen, V.-M., Vasander, H., Nykänen, H., Martikainen, P. J., Laine, J.,
1018 2000. Methane dynamics of a restored cut-away peatland. *Global Change Biology* 6, 569–
1019 581.

1020 Tuittila, E-S., Vasander, H., Laine, J., 2000. Impact of rewetting on the vegetation of a cut-
1021 away peatland. *Applied Vegetation Science* 3, 205-212.

1022 Turetsky, M. R., Treat, C. C., Waldrop, M. P., Waddington, J. M., Harden, J. W., McGuire,
1023 A. D., 2008. Short-term response of methane fluxes and methanogen activity to water table
1024 and soil warming manipulations in an Alaskan peatland. *Journal of Geophysical Research*,
1025 *Biogeosciences* 113(G3).

1026 Urbanová, Z., Pícek, T., Hájek, T., Bufková, I., Tuittila, E. S., 2012. Vegetation and carbon
1027 gas dynamics under a changed hydrological regime in central European peatlands. *Plant*
1028 *Ecology, Diversity* 5(1), 89-103.

1029 Waddington, J. M., Strack, M., Greenwood, M. J., 2010. Toward restoring the net carbon sink
1030 function of degraded peatlands, Short-term response in CO₂ exchange to ecosystem-scale
1031 restoration. *Journal of Geophysical Research, Biogeosciences* 115(G1).

1032 Voigt, C., Lamprecht, R. E., Marushchak, M. E., Lind, S. E., Novakovskiy, A., Aurela, M.,
1033 Martikainen, P. J., Biasi, C., 2017. Warming of subarctic tundra increases emissions of all
1034 three important greenhouse gases—carbon dioxide, methane, and nitrous oxide. *Global*
1035 *Change Biology* 23(8), 3121-3138.

1036 Ward, S. E., Ostle, N. J., Oakley, S., Quirk, H., Henrys, P. A., Bardgett, R. D., 2013.
1037 Warming effects on greenhouse gas fluxes in peatlands are modulated by vegetation
1038 composition. *Ecology Letters* 16(10), 1285-1293.

1039 Weltzin, J. F., Bridgman, S. D., Pastor, J., Chen, J., Harth, C., 2003. Potential effects of
1040 warming and drying on peatland plant community composition. *Global Change Biology* 9(2),
1041 141-151.

1042 Wiedermann, M. M., Nordin, A., Gunnarsson, U., Nilsson, M. B., Ericson, L., 2007. Global
1043 change shifts vegetation and plant–parasite interactions in a boreal mire. *Ecology* 88(2), 454-
1044 464.

1045 Wilson, D., Alm, J., Riutta, T., Laine, J., Byrne, K. A., Farrell, E. P., Tuittila, E. S., 2007. A
1046 high resolution green area index for modelling the seasonal dynamics of CO₂ exchange in
1047 peatland vascular plant communities. *Plant Ecology* 190(1), 37-51.

1048 Wilson, D., Farrell, C. A., Fallon, D., Moser, G., Müller, C., Renou-Wilson, F., 2016.
1049 Multiyear greenhouse gas balances at a rewetted temperate peatland. *Global Change Biology*
1050 22, 4080–4095

1051 Wilson, J. W., 1959. Analysis of the spatial distribution of foliage by two-dimensional point
1052 quadrats. *New Phytologist* 58(1), 92-99.

1053 Vompersky, S. E., Sirin, A. A., 1997. Hydrology of drained forested wetlands. in Trettin, C.
1054 C., Jurgense, M. F., Grigal, D. F., Gale, M. R., Jeglum, J. K. eds. *Northern forested wetlands.*
1055 *Ecology and management.* CRS Press Inc., Lewish Publishers, Boca Raton, FL. pp. 189–211.

1056 Yu, Z., Beilman, D. W., Froking, S., MacDonald, G. M., Roulet, N. T., Camill, P., Charman,
1057 D. J., 2011. Peatlands and Their Role in the Global Carbon Cycle. *Eos Trans. AGU* 92(12),
1058 97.

1059 Yu, Z. C., 2012. Northern peatland carbon stocks and dynamics: a review. *Biogeosciences*
1060 9(10), 4071-4085.

1061

1062 Table 1. Average air and soil temperature (°C) at OTC warming plots and ambient-T plots in
 1063 Undrained, Restored and Drained land use category during spring (May), summer (June-
 1064 August) and autumn (September-November). Statistically significant ($p < 0.05$) differences
 1065 between OTC and Ambient-T plots are marked with * (ANOVA-tests).

		Spring		Summer		Autumn	
		OTC	Ambient-T	OTC	Ambient-T	OTC	Ambient-T
Air T at	Undrained	18.9	16.8*	17.1	15.8*	7.4	6.5*
15cm	Restored	18.7	17.7	17.0	16.3*	7.8	7.1*
	Drained	17.0	16.3	15.9	15.3	7.3	6.9
Soil T at	Undrained	11.4	11.4	14.9	14.6	9.1	8.3
5cm	Restored	11.5	10.8	12.5	12.7	9.4	9.7
	Drained	8.3	8.2	12.5	12.7	8.7	8.5

1066

1067

1068 Table 2. Average annual and summer time temperature (T) and precipitation (Prec) in study
 1069 years 2011 and 2013, and the long-term averages for period 1981-2010. Summer denotes for
 1070 June-August. Data from Siikajoki, Revonlahti weather station, Finnish Meteorological
 1071 Institute and from Pirinen et al. 2012.

Period	T year, °C	T summer, °C	Prec year, mm	Prec summer, mm
2011	4.3	16.0	570	203
2013	4.2	15.4	585	220
30 yr average	2.6	14.2	541	199

1072

1073

1074

1075 Table 3. Mean measured CO₂, CH₄ and N₂O fluxes under different land use and warming
 1076 treatments. UD = undrained, R = restored, D = drained, A = ambient-T, O = OTC warming,
 1077 PG = gross photosynthesis Reco = ecosystem respiration, and NEE = net CO₂ exchange. Unit
 1078 for gas fluxes is mg CO₂/CH₄/N₂O m⁻² h⁻¹. The mean for PG and NEE is based only on light
 1079 saturated measurements with PPFD > 800 μmol m⁻² s⁻¹.

Year	Land use	Warming	PG		NEE		
			@PPFD>800	Reco	@PPFD>800	CH ₄	N ₂ O
All	UD1	A	955	396	496	0.2	
		O	1041	380	594	0.7	
	UD2	A	1115	414	605	0.7	
		O	935	374	490	1.1	
	R1	A	1116	409	517	1.1	
		O	1122	364	613	1.4	
	R2	A	959	374	446	0.6	
		O	919	335	469	0.6	
	D1	A	537	751	-74	0.0	
		O	657	525	141	0.1	
	D2	A	796	337	349	0.4	
		O	830	363	365	0.4	
2011	UD1	A	990	335	591	0.2	0.1
		O	1135	332	756	0.8	0.2
	UD2	A	983	313	609	0.6	0.2
		O	797	317	459	1.3	0.2

	R1	A	826	361	221	1.4	0.2
		O	873	327	417	1.8	0.3
	R2	A	994	363	522	0.8	0.2
		O	995	316	569	0.9	0.3
	D1	A	549	692	-40	0.0	0.2
		O	679	473	166	0.1	0.2
	D2	A	711	316	307	0.5	0.3
		O	628	326	218	0.6	0.2
2013	UD1	A	934	427	440	0.2	
		O	983	406	496	0.6	
	UD2	A	1171	466	604	0.8	
		O	1017	414	509	0.8	
	R1	A	1228	438	631	0.2	
		O	1264	387	725	0.3	
	R2	A	921	382	363	0.4	
		O	839	349	364	0.2	
	D1	A	503	792	-176	0.1	
		O	642	559	124	0.0	
	D2	A	852	352	377	0.1	
		O	980	390	474	0.0	

1080

1081

1082 Table 4. Global warming potential (GWP) of different land uses (UD = undrained, R =
 1083 restored, D = drained) based on gas fluxes calculated for growing seasons 2011 and 2013.
 1084 GWP calculated based on 100-year time horizon (Myhre et al. 2013). The values are
 1085 expressed as g CO_{2-eq} m⁻² season⁻¹ and positive values indicate net warming impact to
 1086 atmosphere. The estimates for drained sites include the annual above-ground tree stand CO₂
 1087 sequestration, which would occur mostly during the growing season.

Study site	GWP_2011	GWP_2013
UD1	156	462
UD2	-114	145
R1	243	516
R2	-137	240
D1	178	334
D2	709	971

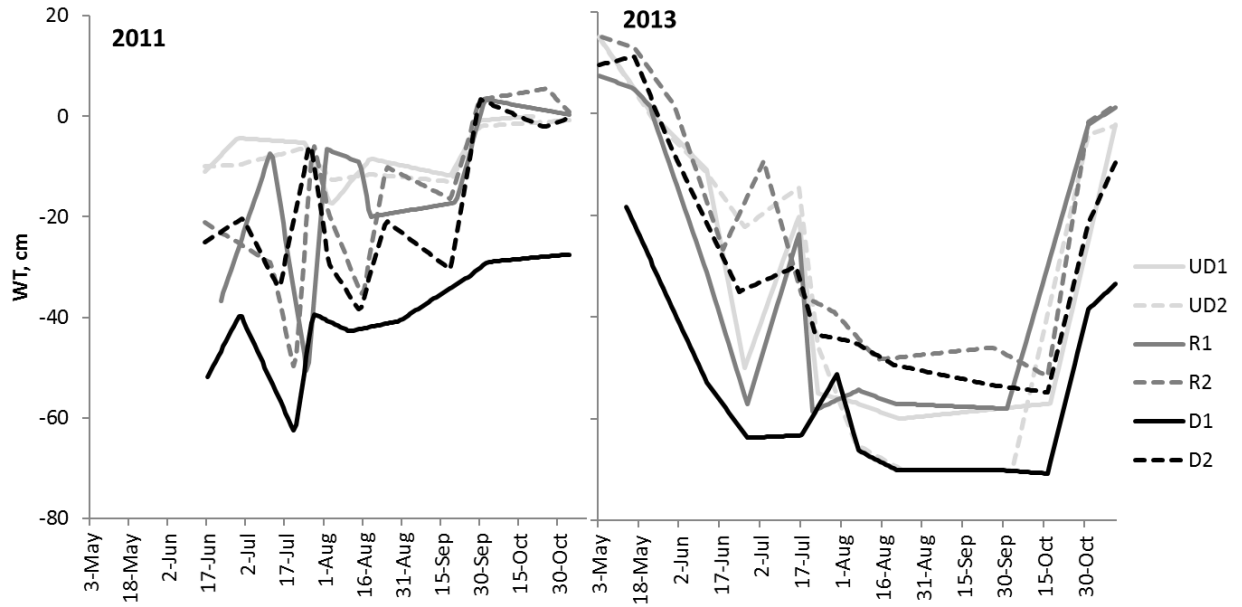
1088

1089

1090 Figures

1091

1092

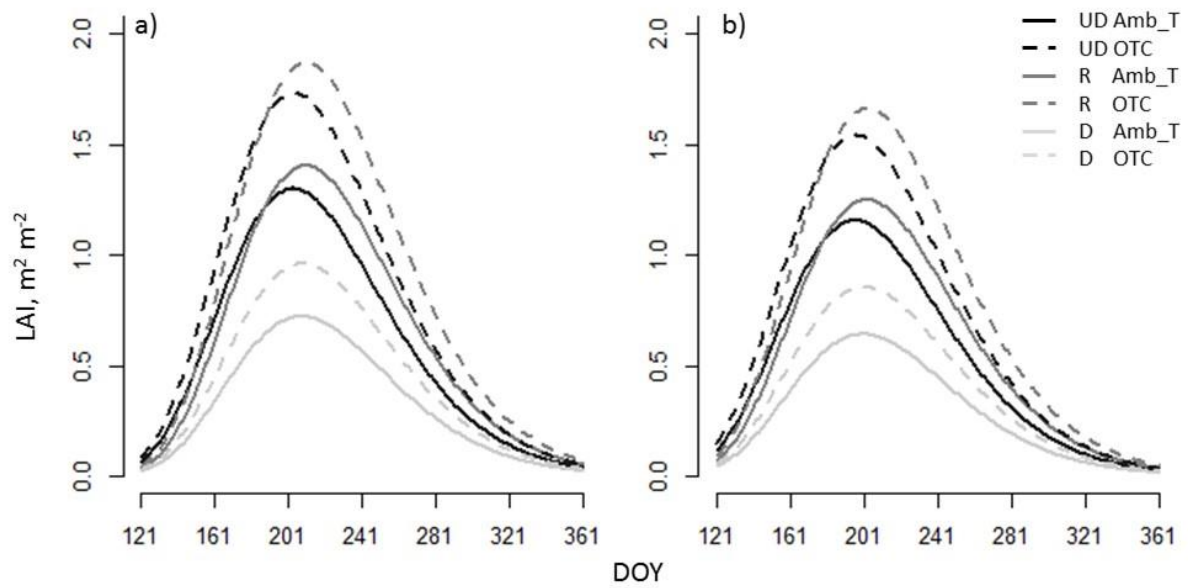


1093

1094 Figure 1. Water table (WT) in years 2011 and 2013 in the six study sites. UD = undrained, R
1095 = restored and D= drained. Values below zero indicate WT below soil surface.

1096

1097

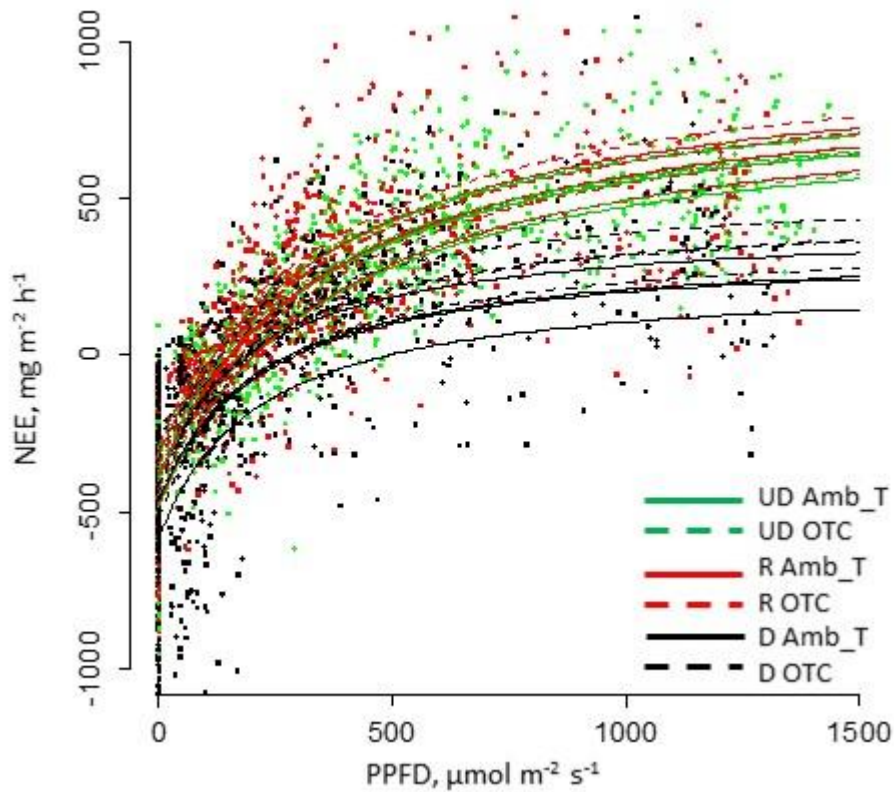


1098

1099 Figure 2. Seasonal development (May to December) of leaf area index (LAI) during a) year
1100 2011 and b) year 2013, in ambient-T (Amb_T, solid lines) and OTC warmed plots (dashed
1101 lines) at undrained (UD), restored (R) and drained (D) sites belonging to Group 1. As LAI of
1102 group 2 behaved at similar manner to group 1, those results are not shown here.

1103

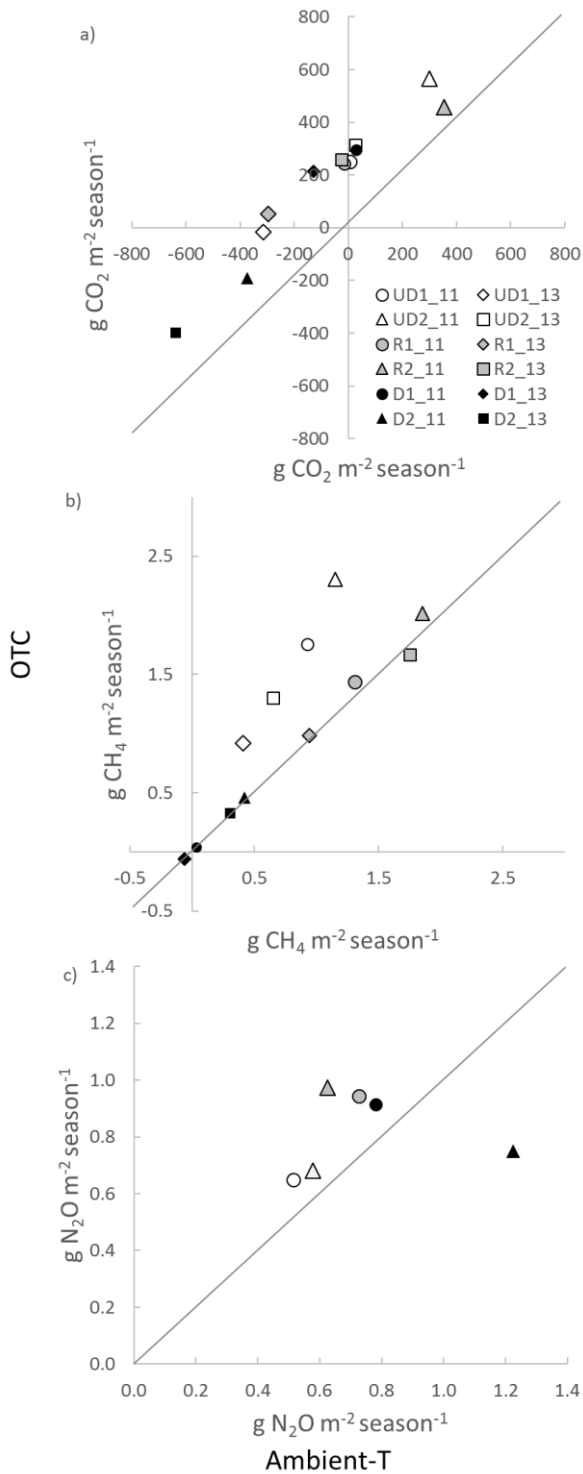
1104



1105

1106 Figure 3. Light response of net ecosystem CO₂ exchange (NEE) under different land use and
1107 warming treatments. Scatter plot shows the measured fluxes, while the different response
1108 curves are based on CO₂ model and represent the three land uses (UD = undrained, R =
1109 restored, D = drained), warming treatments (Amb_T = ambient-T, OTC = OTC warming),
1110 measurement years (2011, 2013) and site groups 1 and 2. Therefore, the four lines per land
1111 use x warming treatment describe the variability caused by year and site group.

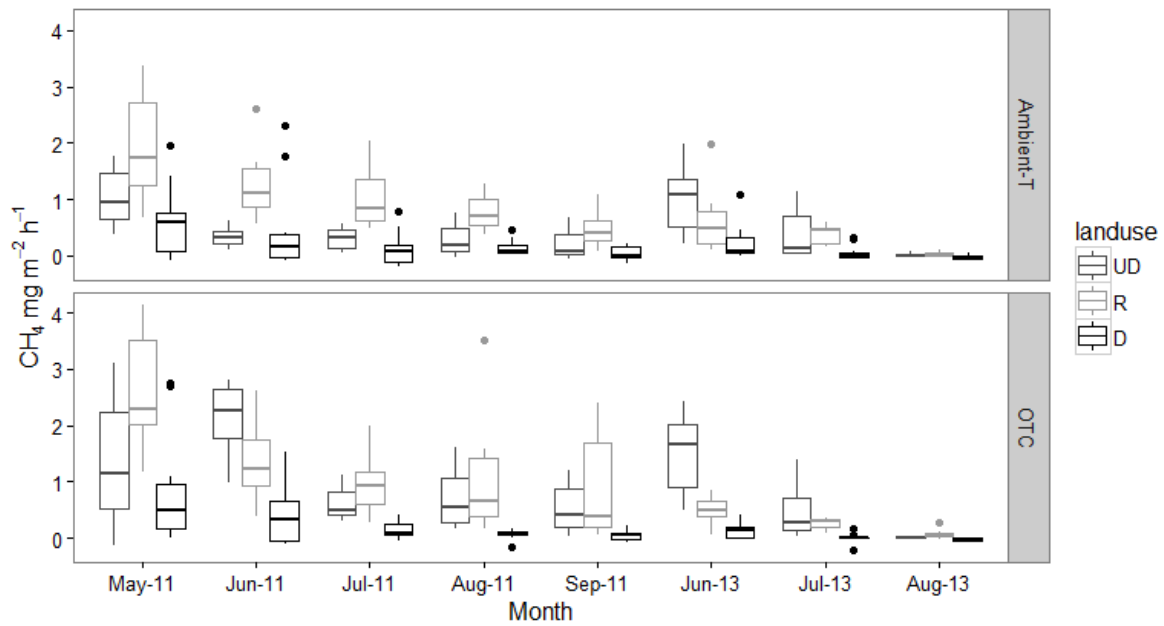
1112



1113

1114 Figure 4. Scatterplot of Ambient-T vs. OTC-warmed seasonal (May-September) cumulative
 1115 flux of a) net ecosystem CO₂ exchange (NEE), b) methane, c) nitrous oxide. Seasonal fluxes
 1116 are calculated for OTC-warmed and ambient-T plots for each study site and for seasons 2011
 1117 and 2013. UD: undrained, R: restored, D: drained. We added the annual average tree stand
 1118 carbon sequestration of 959 and 423 g CO₂ m⁻² to the field layer NEE estimates of sites D1
 1119 and D2, respectively. 1:1 line is shown for each GHG component.

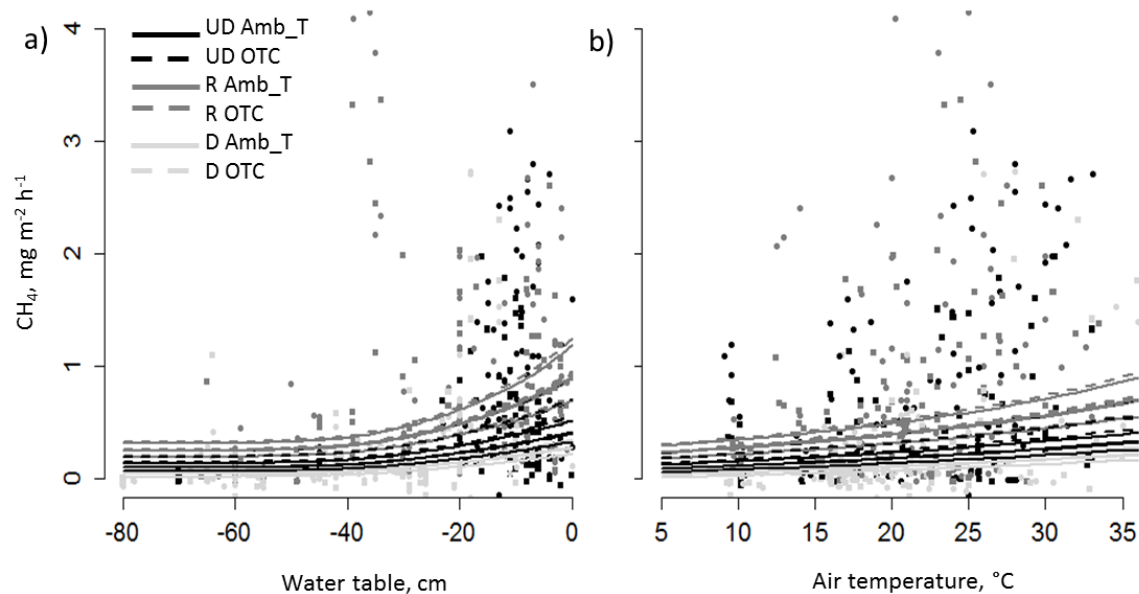
1120



1121

1122 Figure 5. Box-plot of average measured CH₄ fluxes at undrained (UD), restored (R) and drained
 1123 (D) sites under warmed (OTC) or ambient-T (C) temperature during the eight measurement
 1124 campaigns at May, June, July, August and September of year 2011 and June, July and August
 1125 of year 2013. Boxes represent range of middle two quartiles of the data, horizontal line is the
 1126 median, and whiskers show the range excluding outliers (points).

1127



1129

1130 Figure 6. Scatter plot of measured fluxes and response curves from full CH₄ model1131 (Appendix 3). a) CH₄ flux related to water table level and b) to air temperature.

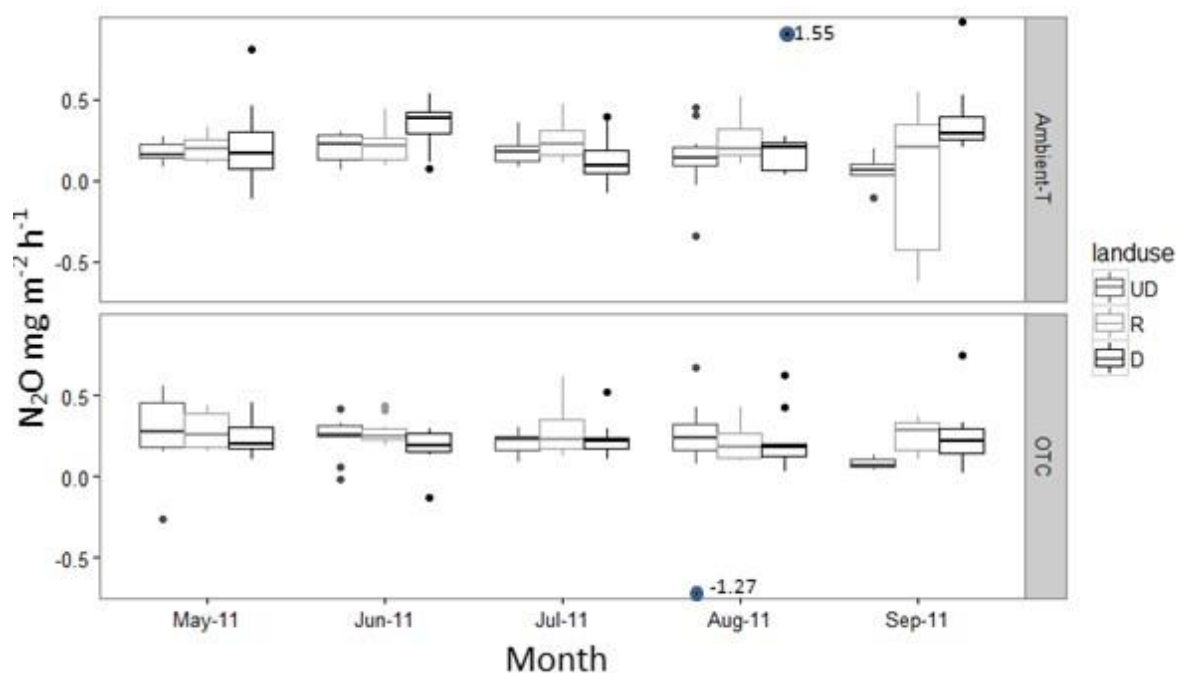
1132 Environmental variables are standardized to following values based on data averages: WT: -

1133 26.5 cm, Ta: 20.79°C, T5: 13.01 °C, field-layer LAI: 1.08 m²m².

1134

1135

1136



1137

1138 Figure 7. Box-plot of N₂O fluxes at undrained (UD), restored (R) and drained (D) sites under
1139 warmed (OTC) or ambient-T (C) temperature during the five measurement campaigns at
1140 May, June, July, August and September of year 2011. At the boxplot, the line that divides the
1141 box into two parts represents the median of the data and the end of the box shows the upper
1142 and lower quartiles. The whickers show the highest and lowest value excluding outliers,
1143 which are represented by points. The two extreme outliers are shown with respective values.

1144

1145

1146

1147 **Supporting information for online publication** **Nonlinear mixed-effect models**
1148 **for leaf area index** and GHG fluxes

1149 Laine et al. Impacts of drainage, restoration and warming on boreal wetland greenhouse gas
1150 fluxes

1151 0000-0003-2989-1591

1152 **Supporting information 1. Nonlinear mixed-effect model based on leaf area index**

1153 **Supporting information 2. Nonlinear mixed-effect model based on CO₂ flux**
1154 **measurements**

1155 **Supporting information 3. Linear mixed effect models based on CH₄ measurements**

1156 **Supporting information 4. Linear mixed effect models based on N₂O measurements**

1157

1158 **Supporting information 1. Nonlinear mixed-effect model based on leaf area index**

1159 Table S1.1. ANOVA results of the non-linear mixed effects models (Eq. 1-3) for the
 1160 differences in leaf area index (LAI) between land use (undrained, drained, restored), warming
 1161 treatment, years (2011 and 2013) and group (two groups of sites: UD1, R1 and D1, and UD2,
 1162 R2 and D2). LMAX is maximum LAI during growing season and DMAX is the day of year
 1163 when maximum is reached.

1164

Source	numDF	denDF	LMAX		DMAX	
			F-value	p-value	F-value	p-value
Year	1	648	8.12	0.005	19.93	<.0001
Land use	2	648	6.7	0.001	5.08	0.006
Warming	1	648	8.64	0.003	0.06	0.803
Group	1	648	1.69	0.194	12.32	0.001

1165

1166 Table S1.2. Parameter estimates and random effects of nonlinear mixed-effects model of leaf
 1167 area index (LAI) model (Eq.1-3). The bolded values are significant at $p < 0.05$. Then drained
 1168 site of group 1 with no warming in year 2011 is used as control.

Source	DF	ln(LMAX)		ln(DMAX)		ln(G) Value	Std Error
		Value	Std.Error	Value	Std.Error		
<i>Fixed part</i>							
Intercept	648	0.26	0.17	5.32	0.01	-1.52	0.121
Year 2013	648	-0.12	0.04	-0.04	0.01		
Restoration	648	0.08	0.20	0.03	0.01		
Drainage	648	-0.59	0.20	0.02	0.01		
Warming	648	0.29	0.10	0.002	0.01		
Group2	648	0.21	0.16	-0.03	0.01		
<i>Random effects and residual</i>							
var(a_i)		0.16 ²		0		0.29 ²	
var(b_{ij})		0.34 ²		0.01 ²		0	
var(c_{ijk})		0.18 ²		0.03 ²		0.08 ²	
var(ϵ_{ijkl})		0.25 ²					

1169

1170 **Supporting information 2. Nonlinear mixed-effect model based on CO₂ flux**
 1171 **measurements**

1172 Table S2.1. ANOVA results of the simple non-linear mixed effects models, including only
 1173 categorical treatments, based on CO₂ measurements (Eq. 4-7).

		numDF	denDF	F-value	p-value
ln(PMAX)	Intercept				
	Year	1	2241	0.03	0.854
	Land use	4	2241	13.46	<.0001
	Warming	3	2241	0.72	0.538
	Group	1	2241	0.19	0.667
	Land use :Warming	2	2241	0.88	0.415
ln(R)	Intercept				
	Year	1	2241	42.75	<.0001
	Land use	4	2241	0.99	0.409
	Warming	3	2241	1.39	0.244
	Group	1	2241	8.15	0.004
	Land use :Warming	2	2241	0.03	0.970
ln(α)	Intercept				
	Land use	2	2241	13.85	<.0001

1174

1175

1176 Table S2.2. Parameter estimates and random effects of the simple nonlinear mixed effect
 1177 model, including only categorical treatments, based on CO₂ measurements (Eq. 4-7). The
 1178 undrained site of group 1 with no warming in year 2011 is used as control.

Fixed part		Value	Std.Error	DF	t-value	p-value
ln(PMAX)	Intercept	7.15	0.06			
	Year2013	0.01	0.03	2241	0.18	0.854
	Restored	0.03	0.07	2241	0.42	0.671
	Drained	-0.43	0.08	2241	-5.68	<.0001
	Warming	-0.02	0.06	2241	-0.36	0.717
	Group2	-0.02	0.04	2241	-0.43	0.667
	Restored : Warming	0.03	0.08	2241	0.36	0.721
	Drained : Warming	0.11	0.09	2241	1.29	0.199
ln(R)	Intercept	6.00	0.10			
	Year2013	0.19	0.03	2241	6.54	<.0001
	Restored	-0.02	0.12	2241	-0.20	0.845
	Drained	0.18	0.12	2241	1.47	0.142
	Warming	-0.08	0.09	2241	-0.96	0.336
	Group2	-0.22	0.08	2241	-2.85	0.004
	Restored : Warming	-0.02	0.12	2241	-0.13	0.899
	Drained : Warming	-0.03	0.12	2241	-0.25	0.804
ln(α)	Intercept)	5.82	0.07			
	Restored	0.08	0.10	2241	0.81	0.420
	Drained	-0.48	0.11	2241	-4.30	<.0001
Random part		PMAX	R	α		
var(a_i)		0.00 ²	0.09 ²	0.06 ²		
var(b_{ij})		0.00 ²	0.16 ²	0.00 ²		
var(c_{ijk})		0.19 ²	0.11 ²	5.42 ²		
var(d_{ijkl})		0.25 ²	0.37 ²	0		
corr(d_{ijkl}^P, d_{ijkl})		1				
var(ϵ_{ijklm})		100.25 ²				

1179

1180

1181

1182 Table S2.3. ANOVA results of the full nonlinear mixed effect model, including
 1183 environmental variables, based on CO₂ measurements (Eq. 4-7). Ta= air temperature, a1 =
 1184 spline component based on a three-knot spline, LAI2 = is the plot level modelled leaf area
 1185 (Eq 1-3) transformed as $\ln(1-\exp(-LAI))$, min(t15, 10) = soil temperature at 15 cm depth,
 1186 log(LAI) = is logarithmically transformed LAI.

	numDF	denDF	F-value	p-value
ln(PMAX)				
Year	1	2235	19.77	<.0001
Land use	4	2235	1.63	0.163
Warming	3	2235	1.08	0.355
Group	1	2235	5.58	0.018
Ta/a1	2	2235	19.87	<.0001
LAI2	1	2235	219.32	<.0001
Land use :Warming	2	2235	0.40	0.669
ln(R)				
Year	1	2235	188.08	<.0001
Land use	4	2235	1.31	0.262
Warming	3	2235	4.42	0.004
Group	1	2235	3.88	0.048
Ta	1	2235	365.16	<.0001
Log(LAI)	1	2235	95.89	<.0001
min(T15, 10)	1	2235	220.53	<.0001
Land use : Warming	2	2235	0.40	0.670
ln(α)				
Land use	2	2235	7.72	0.001

1187

1188

1189 Table S2.4. Parameter estimates and random effects of the full nonlinear mixed effect model,
 1190 including environmental variables, based on CO₂ measurements (Eq. 4-7). The undrained site
 1191 of group 1 with no warming in year 2011 is used as the control.

Fixed part		Value	Std.Error	DF	t-value	p-value
ln(PMAX)	Intercept	6.88	0.13			
	Year2013	0.15	0.03	2235	4.45	<.0001
	Restored	-0.01	0.11	2235	-0.05	0.961
	Drained	-0.16	0.11	2235	-1.43	0.152
	Warming	-0.08	0.08	2235	-0.95	0.343
	Group2	-0.15	0.06	2235	-2.36	0.018
	Ta	0.03	0.01	2235	6.29	<.0001
	a1	0.00	0.00	2235	-5.68	<.0001
	LAI2	0.65	0.04	2235	14.81	<.0001
	Restored :Warming	0.05	0.11	2235	0.47	0.641
	Drained : Warming	-0.05	0.12	2235	-0.44	0.663
ln(R)	Intercept	4.02	0.18			
	Year2013	0.28	0.02	2235	13.71	<.0001
	Restored	-0.06	0.22	2235	-0.27	0.789
	Drained	0.39	0.22	2235	1.82	0.069
	Warming	-0.14	0.09	2235	-1.61	0.106
	Group2	-0.17	0.09	2235	-1.97	0.049
	Ta	0.03	0.00	2235	19.11	<.0001
	Log(LAI)	0.24	0.02	2235	9.79	<.0001
	Pmin(T15,10)	0.14	0.01	2235	14.85	<.0001
	Restored: Warming	-0.01	0.12	2235	-0.08	0.935
	Drained: Warming	-0.10	0.12	2235	-0.81	0.418
ln(α)	Intercept	5.65	0.09			
	Restored	0.14	0.13	2235	1.14	0.254
	Drained	-0.38	0.13	2235	-2.80	0.005
Random part		PMAX	R	α		
var(a_i)		0.06 ²	0.20 ²	0.1 ²		
var(b_{ij})		0.13 ²	0.18 ²	0.00 ²		
var(c_{ijk})		0.17 ²	0.04 ²	0.25 ²		
var(d_{ijkl})		0.23 ²	0.19 ²			
corr(d_{ijkl}^P, d_{ijkl})			0.58 ²			
var(ϵ_{ijklm})			78.41			

1192

1193

1194 **Supporting information 3. Linear mixed effect models based on CH₄ measurements**

1195 Table S3.1. ANOVA results of the simple linear mixed effect model, including categorical
 1196 treatments, based on CH₄ measurements, using the transformation $-1/(CH_4 + 0.4)$.

	Sum Sq	mean Sq	NumDF	DenDF	F.value	Pr(>F)
Year	0.66	0.66	1	6.02	2.43	0.170
Land use	2.29	1.14	4	2.48	3.78	0.182
Warming	1.15	1.15	3	51.86	3.65	0.018
Group	0.27	0.27	1	0.00	0.98	
Land use:Warming	1.86	0.93	2	51.84	3.39	0.041

1197

1198 Table S3.2. Parameter estimates and random effects of the simple linear mixed effect model,
 1199 including categorical treatments, based on CH₄ measurements. Measurements from the
 1200 undrained site of group 1 with no warming in year 2011 are used as the control.

Fixed part	Estimate	Std.Error	df	t	p value
Intercept	-1.49	0.36			
Year 2013	-0.50	0.32	6.0	-1.56	0.170
Restored	0.40	0.38	2.2	1.06	0.395
Drained	-0.61	0.38	2.2	-1.62	0.237
Warming	0.35	0.11	51.7	3.30	0.002
Group2	0.30	0.30	2.0	0.99	0.427
Restored : Warming	-0.33	0.15	52.7	-2.18	0.034
Drained : Warming	-0.35	0.15	50.9	-2.32	0.024
Random part	Variance				
site	0.36 ²				
plot:site	0.15 ²				
mestime	0.43 ²				
Residual	0.52 ²				

1201

1202

1203 Table S3.3. ANOVA results of the full linear mixed effect model, including environmental
 1204 variables, for CH₄ measurements (-1/CH₄+0.4). LAI_S = is the modelled plot level leaf area
 1205 including only sedges (Eq 1-3), WT = water table, a1 = the second term of the three-knot
 1206 spline for WT, Ta= air temperature, T5 = soil temperature in 5 cm depth.

	Sum Sq	mean Sq	NumDF	DenDF	F.value	Pr(>F)
Year	0.06	0.06	1	7	0.247	0.635
Land use	1.04	0.52	4	2.7	3.224	0.195
Warming Group	0.83	0.83	3	51	3.923	0.013
LAI_S	0.06	0.06	1	2	0.257	0.662
WT and a1	0.62	0.62	1	229	2.494	0.116
	0.05	0.05	2	410	12.158	<.0001
Ta	1.56	1.56	1	373	6.234	0.013
T5	0.18	0.18	1	432	0.704	0.402
Land use:Warming	1.43	0.71	2	50	2.859	0.067

1207

1208 Table S3.4. Parameter estimates and random effects of the full linear mixed effect model
 1209 including environmental variables, based on CH₄ measurements. Measurements from
 1210 undrained site of group 1 with no warming in year 2011 are used as the control.

Fixed part	Estimate	Std.Error	df	t	p value
Intercept	-2.55	0.54			
Year2013	-0.13	0.27	7	-0.50	0.635
Restored	0.46	0.36	2	1.28	0.320
Drained	-0.25	0.36	2	-0.68	0.558
Warming	0.32	0.11	52	2.97	0.005
Group2	0.15	0.29	2	0.51	0.662
LAI_S	0.11	0.07	230	1.58	0.116
WT	0.00	0.01	404	0.45	0.653
a1	0.00	0.00	416	1.83	0.069
Ta	0.02	0.01	373	2.50	0.013
T5	0.02	0.02	432	0.84	0.402
Restored: Warming	-0.30	0.15	52	-1.95	0.057
Drained: Warming	-0.33	0.15	49	-2.18	0.034
Random part	Variance	.			
site	0.34 ²				
plot:site	0.16 ²				
mestime	0.34 ²				
Residual	0.50 ²				

1211 **Supporting information 4. Linear mixed effect models based on N₂O measurements**

1212 Table AS.1. ANOVA results of the simple linear mixed effect model, including only
 1213 categorical treatments, for N₂O measurements.

	Sum Sq	mean Sq	NumDF	DenDF	F.value	Pr(>F)
Land use	0.17	0.09	4	284.12	2.74	0.029
Warming	0.11	0.11	3	284.12	2.96	0.033
group	0.02	0.02	1	284.33	0.56	0.455
Land use:Warming	0.14	0.07	2	284.14	2.46	0.087

1214

1215 Table S4.2. Parameter estimates and random effects of the simple linear mixed effect model,
 1216 including only categorical treatments, based on N₂O measurements. Measurements from
 1217 undrained site of group 1 with no warming in year 2011 are used as the control.

Fixed part	Estimate	Std.Error	df	t	p value
Intercept	0.14	0.03			
Restored	0.04	0.03	284.11	1.03	0.302
Drained	0.10	0.03	284.19	2.90	0.004
Warming	0.06	0.03	284.11	1.80	0.073
group2	0.01	0.02	284.33	0.75	0.455
Restored :Warming	0.02	0.05	284.08	0.32	0.751
Drained :Warming	-0.08	0.05	284.21	-1.74	0.084
Random part	Variance				
site	0				
plot:site	0				
meastime	0.02 ²				
Residual	0.17 ²				

1218

1219

1220 **Table S4.3.** ANOVA results of the full linear mixed effect model including also
 1221 environmental variables for log transformed N₂O measurements. WT = water table, Ta= air
 1222 temperature and LAI = is the modelled plot level leaf area (Eq 1-3),

	Sum Sq	mean Sq	NumDF	DenDF	F.value	Pr(>F)
Land use	0.100	0.050	4	285	2.07	0.084
Warming	0.086	0.086	3	285	2.53	0.058
Group	0.020	0.020	1	285	0.68	0.409
WT	0.012	0.012	1	285	0.41	0.525
Ta	0.052	0.052	1	285	1.82	0.178
LAI	0.017	0.017	1	285	0.61	0.437

1223

1224 **Table S4.4.** Parameter estimates and random effects of the full linear mixed effect model
 1225 including environmental variables, based on log transformed N₂O measurements.
 1226 Measurements from undrained site of group 1 with no warming in year 2011 are used as the
 1227 control.

Fixed part	Estimate	Std.Error	df	t	p value
Intercept	0.085	0.040			
Restored	0.033	0.034	285	0.97	0.333
Drained	0.094	0.040	285	2.33	0.020
Warming	0.061	0.035	285	1.73	0.084
Group2	0.018	0.021	285	0.83	0.409
WT	-0.001	0.001	285	-0.64	0.525
Ta	0.002	0.001	285	1.35	0.178
LAI	0.012	0.015	285	0.78	0.437
Restored :Warming	0.011	0.048	285	0.22	0.828
Drained :Warming	-0.085	0.049	285	-1.76	0.080
Random part	Variance				
site	1.74E-08 ²				
plot:site	0.00E+00 ²				
meastime	0.00E+00 ²				
Residual	1.69E-01 ²				

1228

1229